Imperial College London

Using Deep Learning to Identify Cyclists Risk Factors in London

MRes Biomedical Research (Data Science)

Luís Rita

Supervisors: Majid Ezzati & Ricky Nathvani

20 August 2020

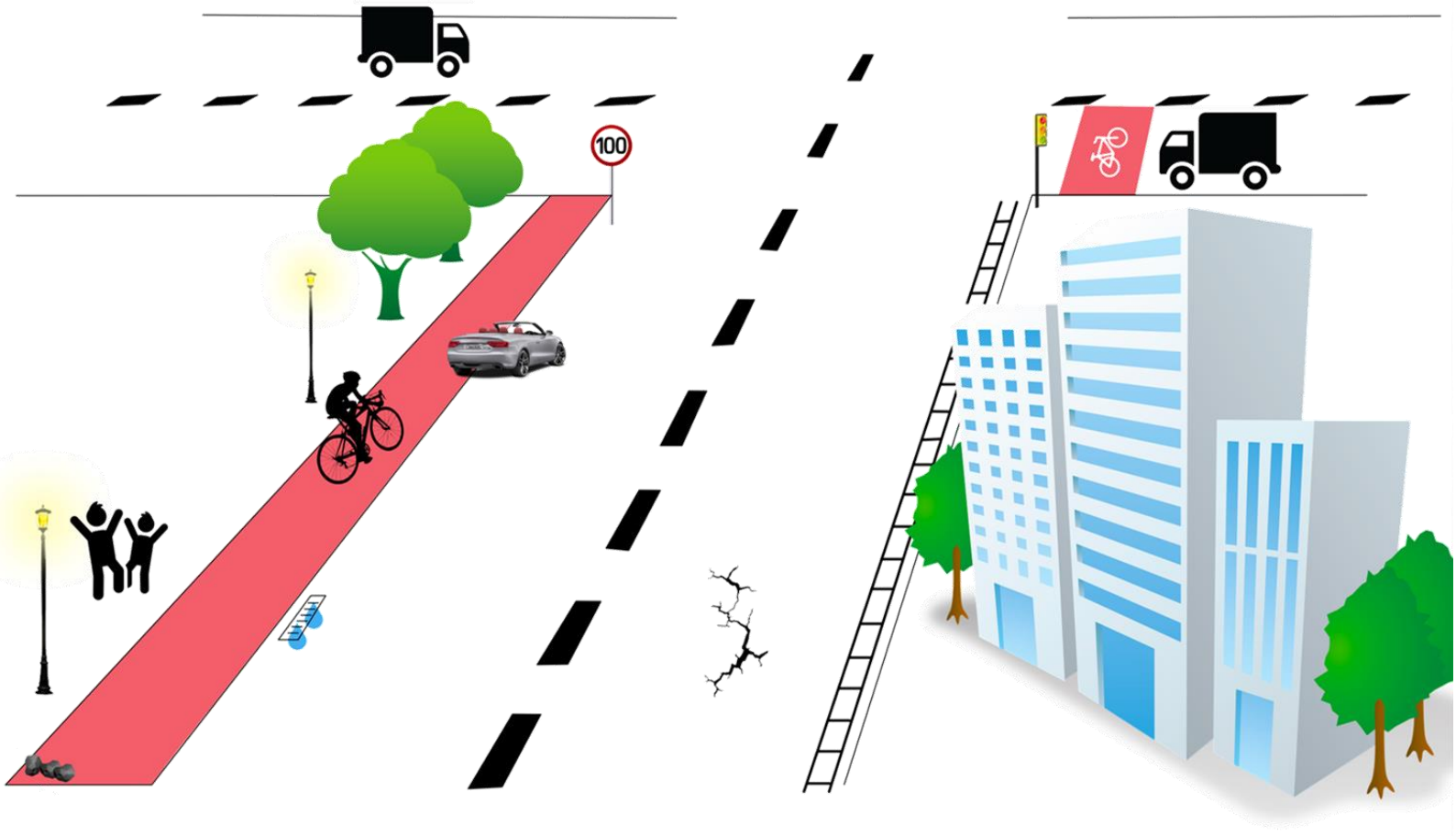

I certify that this thesis, and the research to which it refers, are the product of my own work, conducted during the current year of the MRes in Biomedical Research at Imperial College London. Any ideas or quotations from the work of other people, published or otherwise, or from my own previous work are fully acknowledged in accordance with the standard referencing practices of the discipline.

Luís Rita

Abstract

Cycling encompasses many societal benefits. It influences community safety, economy, environment, equity and health. Number of cyclists on the roads is highly influenced by their perception of safety. To determine road safety, it is fundamental to have a clear metric. For example, consisting in a combination of accident, injury or fatality rates. This will allow the ranking of cyclist's risk factors.

The aim of this project was to use object detection and image segmentation models to extract cyclists' road risk factors from a Google Street View (GSV) imagery of London. This included compiling all risk factors and road safety indicators involved. Using two state-of-the-art tools, YOLOv5 and PSPNet101, pretrained in MS Coco and Cityscapes datasets, respectively, to detect all objects and segment images accordingly to the categories available in the two previous datasets. Finally, after analysing the geographical distribution of the available images in

YOLOv5 was

PSPNet101

After executing YOLOv5 and PSPNet101 in the GSV dataset, it was shown the potential of this type of datasets for the study not

RESULTS

Future developments include increasing the availability of GSV images in the areas surrounding Central London. Combine object detection and image segmentation results at a road level. And to define a metric able to estimate road safety based on these two.

Deep Learning | Cyclists Risk Factors | London

Acknowledgments

Deeply grateful to my supervisors Majid Ezzati and Ricky Nathvani. And all others from Imperial's School of Public, including Barbara Metzler, Emily Muller and Esra Suel. Kavi Bhalla (University of Chicago), Jill Baumgartner (McGill University) and Michael Brauer (University of British Columbia) have importantly contributed.

☆ Dimitris ☆Jordi

Table of Contents

List of Figures

List of Tables

1. Introduction

This section starts with an overview on the most important societal benefits associated to cycling. Then, road safety indicators are introduced so that a clear ranking on the most relevant cyclist's risk factors could be established. Available datasets with relevant objects or segmented images in the context of this project are presented. One object detection and another image segmentation model are described.

1.1. Cycling Benefits

Cycling comprehends multiple benefits to society. They can be categorized in 5 main domains: Safety, Economy, Environment, Equity and Health [1].

The main cause of death in the USA in youngers was traffic accidents. Accounting for 41% of the total number of deaths in the age group 15 to 24 [CDC]. In the European Union, in the past 10 years, deaths among cyclists remained constant, while for car drivers and passengers had decreased 24%. Among pedestrians fell by 19% (Figure 1). UK was one of the only 3 EU nations which fatality rate among pedestrians increased, 1.3% a year. On average, it fell 2.6% in EU per year. For cyclists, in the UK, the number of fatalities decreased 1.3%, with the 13th-best average annual drop. Given that 99% of the pedestrians killed were struck by motor vehicles and 1% by bikes, it is evident the necessity of promoting cyclists' safety and increase their number in the streets. In parallel, this promotes safety in numbers: cyclists are safer if their number increases. The awareness drivers develop by contacting more frequently with cyclists is the root cause.

Many economic benefits for individuals, companies and communities are known from promoting walking and cycling as alternative ways of transportation (Figure 2). According to 2015 Urban Mobility Scorecard, the cost of congestion for the US in 2014 was 160 billion dollars. For an individual was estimated to be 960 dollars each year. These values account for time and fuel expenses. While the cost of having a car in the USA in 2018 was calculated to be 8849 dollars, for a bike was 308 dollars and walking was considered free. 2018 Benchmarking Report adds that bike tourism has a positive economic impact in multiple regions worldwide. Protected Bike Lanes Mean Business Report shows the positive impact cycling may have in business.

It was found that workers doing their commutes cycling, on average, spent more time and travelled more often to their companies, then car drivers. Moreover, in a 2011 study, the Political Economy Research Institute found that 11.41 jobs were on average created when investing 1 million pounds in bicycle-only projects, comparing to 7.75 jobs while investing the same amount in road-only projects.

Reducing the dependency on non-renewable sources, it is also one of the positive aspects of cycling. It was estimated by the United States Environmental Protection Agency that the transportation sector was responsible by the largest share of greenhouse gas emissions – 28% (in the USA). From those, passenger vehicles and light-duty trucks account for most of the overall transport sector – 60%. Moreover, it is also known that structures such as roads and parking lots increase significantly the probability of urban flooding, stormwater runoff and urban heat island effect (due to the lack of shadows and exposed land in the cities, they often register higher temperatures than the surroundings, resultant from the low levels of air humidity). Promoting cycling will reduce the need of the previous infrastructures and mitigate some of the consequences.

Promoting cycling among the population of a country promotes equity. Due to the high cost of car ownership, when a city prioritizes road infrastructure for these vehicles, it puts in higher risk low-income families that cannot afford it. This is particularly important in low-income communities where a brief from Bridging the Gap estimated that only 50% of the roads have sidewalks, comparing to 90% in high-income homologous. This results in higher threat for pedestrians and cyclists. The New Majority: Pedalling Towards Equity reported that 26% of people of colour would like to cycle but do not do it due to safety concerns, comparing to 19% in white respondents.

Physical activity, such as cycling and walking, has numerous benefits to physical and mental health (Figure 3). Centre for Disease Control and Prevention reported that 1 in 10 premature deaths, 1 in 8 breast cancers, 1 in 8 cases of colorectal cancer, 1 in 12 people suffering from diabetes and 1 in 15 cases of heart disease could be prevented if citizens became more active. It can also reduce the risk for coronary heart disease, stroke and many respiratory chronic diseases, which are intimately related to air quality. 2018 State of the Air report states over 133.9 million Americans live in counties with unhealthy levels of ozone and/or particle pollution. A factor that is highly influenced by the transportation patterns inside a community. Vehicles are one

of the main contributors accordingly to the United States Environmental Protection Agency. Due to all these benefits, it becomes evident the importance of promoting a less sedentary lifestyle among the population.

For this reason, by promoting cyclists' safety, the whole society will benefit. Cyclists and pedestrians will be safer. Drivers will reduce their commute times and translate that into society gains such as lower levels of pollution and economic losses.

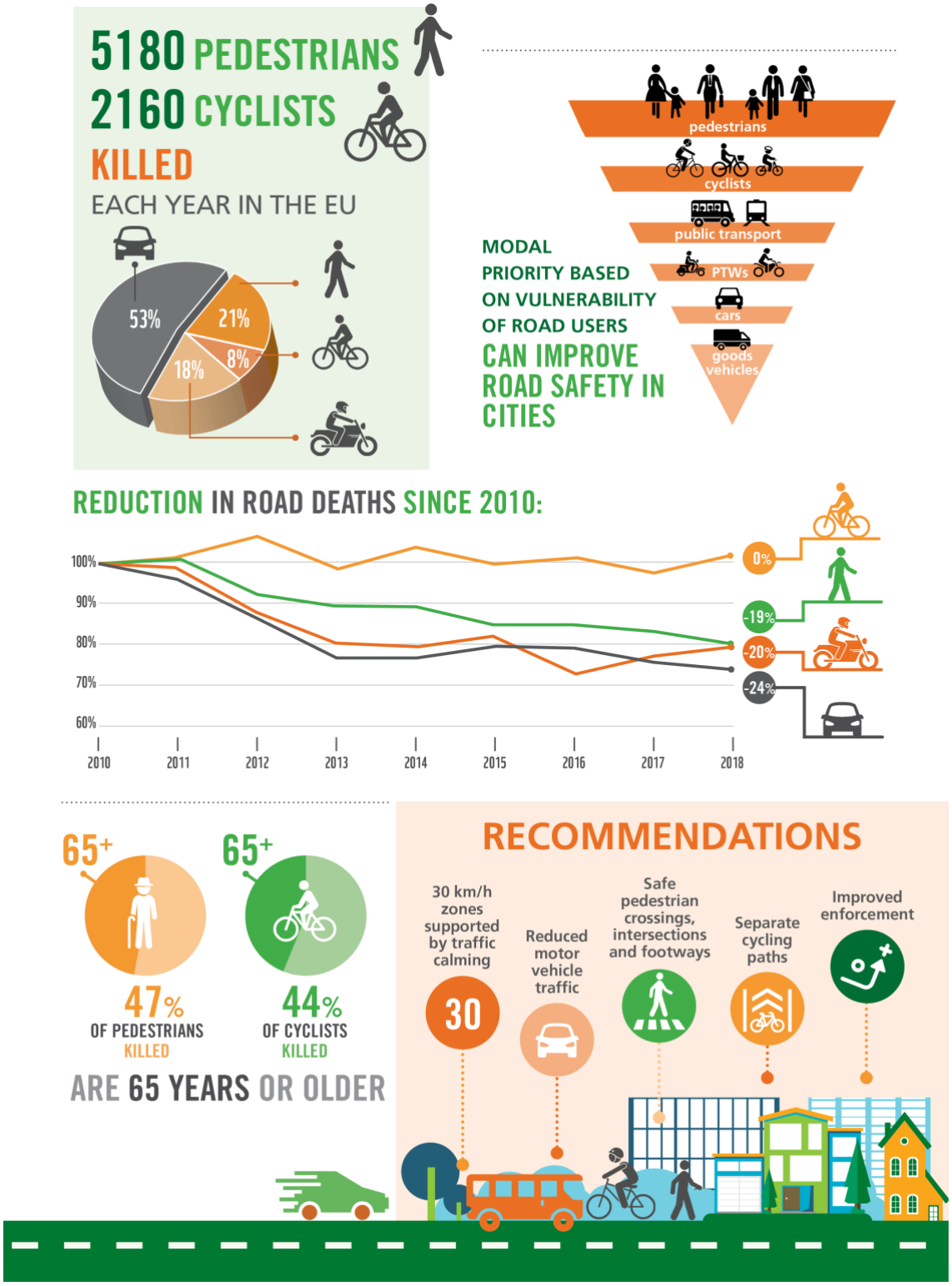

Figure 1 Road safety in EU countries. Accounting for the fact pedestrians and cyclists are the 2 most vulnerable elements on the roads (upper right corner), new safety measures should focus on them. [2]

Figure 2 Sedentarism increases the chance of developing chronic diseases (top). There is a high burden associated with the lack of physical activity (bottom). Adapted from [3].

Figure 3 Impact of physical activity in the risk of premature death (top). Benefits of maintaining an active lifestyle in different stages of life (middle). In a higher scale, communities also benefit from having physically active citizens (bottom). [3]

1.2. Road Safety Indicators

Road safety indicators are essential for policy making. According to the European Road Safety Charter, they allow us to assess the current situation of the roads, observe the impact on accident rates after an intervention, monitor its progress over time and predict further evolutions.

To be useful, road safety indicators should comply with several criteria:

1. Relate to some aspect of road safety, such as the causes or consequences of a road accident.
2. Be Measurable in a reliable way.
3. Be Monitorable over time.
4. Allow road safety engineers or public health experts to set targets.
5. Be Useful for establishing comparisons and benchmarking different safety performances.

There are 6 dimensions common to all indicators: geographical scope, time span, numerical format, representation/visualization, reliability, accuracy, representativeness and a specific "level" of road safety. The first encompasses where the measurement takes place: organisation, city, region, country, Europe or global. The second relates to the time frame comprehensive to the analysis: day, week, month, quarter, year, decade or longer. The units of the measure are represented by the third feature. They can be a proportion, a percentage or some other well-defined ratio. Representation described the way in which data is presented, e.g. in the form of a map, graph or table. Reliability, accuracy and representativeness are linked to the design and implementation of the measurement system. Finally, the "level" of the indicator differs on whether it considers one of the following: impact of the crashes, post-crash response, crash outcomes, crash causes and predictors, road safety policy and measures, or safety culture and safety systems.

Crash outcomes, including indicators such as mortality, severely/slightly injured and accident rates, were the ones considered while selecting the risk factors presented in the next section.

1.3. Risk Factors

14 cyclist risk factors were identified on the roads of London. Table 1 lists them, along with an estimated score proportional to their suitability to be captured using image segmentation and object detection deep learning models. Google Street View images are used for the project. Different tiles were previously prepared to guarantee visual uniformity.

Table 1 Complete list of risk factors identified as relevant while cycling on the roads of London.

Risk Factor	Street View Imagery Suitability	References
Cycle Lane	★★★★★	[4] [5]
Streetlight	★★★★★	[6]
Pedestrians (e.g.: children near schools)	★★★★★	[7]
Water Drainers	★	[7]
Tram/Train Rails	★	[8] [9]
Number Intersections	★★★	[7]
Intersections Visibility	★	[5]
Bends Visibility	★	[5]
Vehicle Speed	★★★★	[4] [7]
Parked Cars	★★★★★	[5] [8] [7]
Lorries and other Large Vehicles	★★★	[8] [7]
Road Width	★★★★	[8]
Pavement Quality (Pits, Trenches, Tree Root Encroachments)	★	[5] [7] [9]
Advanced Stop Line	★	[8] [7]

In an attempt to list and order the most relevant risk factors while cycling in London, I considered the accident, injury and fatality rates. In London, the fatality rate for cyclists is relatively low, consequently, priority was given to the other two more discriminative ones (accident and injury rates). This way, a comparable quantity was used to order all risk factors when designing Figure 4 diagram. Note there is also a strong qualitative and experience-based component inherent to the same rankings.

The top 3 most relevant factors identified to influence cyclists' safety were the presence of a cycle lane, road speed limits and road lane width. Next, statistical data that supports the rankings defined in Figure 4 will be provided. Note that only a small number of accidents involving cyclists are reported [10], consequently, the statistics presented in the next paragraphs may not totally reflect a real-life scenario.

1.3.1. Cycle Lane and Parked Cars

Cycle lanes can be physically separated or located on the road. Depending on the situation, one can be more beneficial than the other.

Physically separated lanes reduce the probability of crash when a car tries to overtake a cyclist or, in the case of fall, to be hit. One of the main causes of injury among cyclists are falls caused by bad pavement quality [5] [7] [9]. With no cars parked in the surroundings, these lanes reduce the risk of injury among cyclists by half. [11] For all these reasons, risks specifically associated to high road speed limits, narrow bicycle lane widths, road pavement quality and parked cars were not considered.

In the case of an on-road cycle lane, vehicular speeds tend to be lower and there are less interactions between these and the cyclists, when comparing to no lane. [12] Near intersections and in roundabouts, some studies suggest these lanes can be safer than physically separated ones. Although, the former can still perform better than the latter if built following specific criteria to make clearly visible the cyclists.

This makes the first scenario the safest, followed by on-road and no cycle lane.

The presence of a cycle lane was considered the most decisive factor by preventing many of the previously identified risks. It was considered the number one in the rankings of risk factors.

1.3.2. Vehicle Speed

Speed was found to be one of the major contributing factors in around 10% of all accidents and 30% of the fatal ones. Speed of vehicles involved in a crash is the single most important factor in determining the severity of injuries. [13]

There are 2 distinct factors when considering speed. Not only higher speeds are known to be responsible for an increased rate of accidents, injuries and deaths, but also large speed differences. Roads with high speed variance are more unpredictable, once they favour the number of encounters and an increased number of overtaking manoeuvres. Consequently, reducing speed limits sometimes may only result in the decrease of the vehicles' average speed and not its variance. [14]

In the core of the danger posed by vehicles' high speeds are the increase in the braking distance and kinetic energy that is transferred from the vehicle to the cyclist. Once both increase with the square of the velocity, the possibility of avoiding or surviving a crash decreases faster than linearly. [14]

In a biological perspective, it is known the human body can only resist the transference of a limited amount of kinetic energy in a crash. [15] This amount varies for different body parts, age groups and gender. Considering the best-designed car, if the vehicle exceeds 30 km/h, this limit can be exceeded. [16] Studies also show if a car travels at a speed lower than 30 km/h, the probability for a pedestrian to survive a crash is higher than 90%. When hit by a car at 45 km/h, the chance of surviving decreases to 50%. [17] Or, as the speed of a car rises from 30 km/h to 50 km/h, the probability of surviving a crash decreases by a factor of 8. [18] In the driver's perspective, the best-designed car provides protection until 70 km/h in frontal collisions where all passengers are wearing belts. [16] For side impacts, the maximum supported velocity is 50 km/h. [16]

In a road safety scope and based on a work done by Nilsson in Sweden, a change in the average speed of 1% for a 120 km/h road would imply a 2% increase in the accident numbers. At 50 km/h, this accident rate would increase instead 4%. In the United Kingdom, in urban roads, an increase of 1 km/h in speed was shown to raise the number the number of accidents by 1 to 4%, depending on the quality of the road. [14]

This was considered the second most relevant factor. In the case of an on-road cycle lane next to a low-speed limit road, the risk factors related to parallel traffic were considered negligible, regardless of the width of the lane.

1.3.3. Lane Width

In the United Kingdom, recommended cycle lane width is 2 meters. Minimum required is 1.5 meters. All values below 1.5 m are considered too narrow, allowing little room to manoeuvre around obstacles, such as: debris, potholes and water drainers. It is frequently referred it is safer not having a bicycle lane, than one that is too narrow, once motorists tend to drive right up to the line and cyclists too close to the kerb.

After the road speed limits, cycle lane width was considered the following most important factor. Whenever it is considered wide, traffic risk factors were not considered. Regardless of the width of an on-road cycle lane, low-speed limits were enough to discard all traffic related risk factors.

1.3.4. Streetlight

After the top 3, streetlight was considered the most relevant criterion in determining road safety. It is known to affect drivers and cyclists' reaction time and make cyclists unnoticeable particularly when not using any reflective or luminous gear. Moreover, in the cyclists' perspective, they are less aware of other road risks associated for example to the quality of the pavement. It is not expected to encounter many significantly under illuminated roads in London, consequently, it was placed in fourth place of the ranking.

1.3.5. Pavement Quality, Tram/Train Rails and Water Drainers

As frequently referred in the literature, pavement quality is a crucial factor to consider when evaluating safety. [5] [7] [9] Pavement quality refers to the quality of the road when there is no cycle lane or to the cycle lane itself, when it is present. Along with the presence of water drainers and trails, these were the following most important risk factors. This was placed under streetlight once with enough luminosity and circulating at a moderate velocity, it may not pose a significant threat.

1.3.6. Number Intersections and Intersections Visibility

The majority of bike and car crashes occur in intersections. In [19], the reported percentage was 60% over the total number of crashes. Additionally, as part of the same study, intersections where streets do not meet at right angles, posed an additional danger to cyclists. Crashes at these areas were 31% more likely to cause serious injury to the cyclist. The main reason is the decreased intersection visibility.

1.3.7. Lorries and other Large Vehicles

In the last years, economic development and consumer demand have been increasing, and so as the number of trucks in the cities. [20] [21] While cycling has following the same trend, the number of encounters among them has significantly increased. As an example, in New York City, 15% of bicycle networks overlap with 11% of truck networks. [22] The increased number of encounters has contributed to a higher accident and mortality rates involving trucks. Truck-bicycle accidents have usually more severe consequences than any other type of accidents. [23] [24] [25] [26] In some EU countries, 30% of all cycling fatalities are associated to trucks. [27] Studies in the past 2 decades have identified trucks as the most common vehicle category involved in cyclist deaths, in London. [24] [28] [29]

1.3.8. Advanced Stop Line

These lines present in several European countries such as Belgium, Denmark and United Kingdom, allow a head start to certain types of vehicles (namely, bicycles) when the traffic signal changes from red to green. This has several advantages. First, drivers behind the line can clearly realize the presence of cyclists around them and take the right precautions to avoid danger manoeuvres. Second, it becomes safer for a cyclist to turn to the left avoiding a crash with the cars that are behind. In terms of statistical data on accident, injury and mortality rate, there is few available.

1.3.9. Bend Visibility

Several sources identify bends as a risk factor. Bends and intersections are often jointly considered as posing similar risks to the cyclist. Namely, low visibility in the cyclist's perspective, make several situations risky that usually are not (sudden appearance of pedestrians or intrusive vegetation). In the driver's perspective, it can be harder to notice cyclist's presence and, consequently, collide against them. [5]

Nevertheless, there is no clear statistical data showing how bends affect cyclists' accident, injury or fatality rates.

1.3.10. Pedestrians

Among all age-groups, pedestrian fatalities most often occur in children younger than 14 years old, when comparing with adults aged between 15 and 64 or 65 or more. In terms of gender, men are at a greater risk than women. [30] For these reasons, locations with higher concentration of people satisfying these criteria (e.g., school areas) are an additional risk. Nevertheless, in car-free zones, accidents between pedestrians and cyclists are extremely rare and almost never serious. [31] Thus, this was considered the least important of the risk factors.

1.3.11. General Overview

Generally, from the left to the right of the diagram the number of risk factors decreases. The most unsafe situation was considered to be no cycle lane. Secondly, high speed limits with a narrow lane in an on-road scenario. Thirdly, high-speed limits but with a wider lane. Fourthly, low-speed limits regardless of the presence of a narrow or wide on-road lane. Finally, a physically separated lane was considered the safest scenario. In red are highlighted the top 3 most relevant factors for each of the different scenarios.

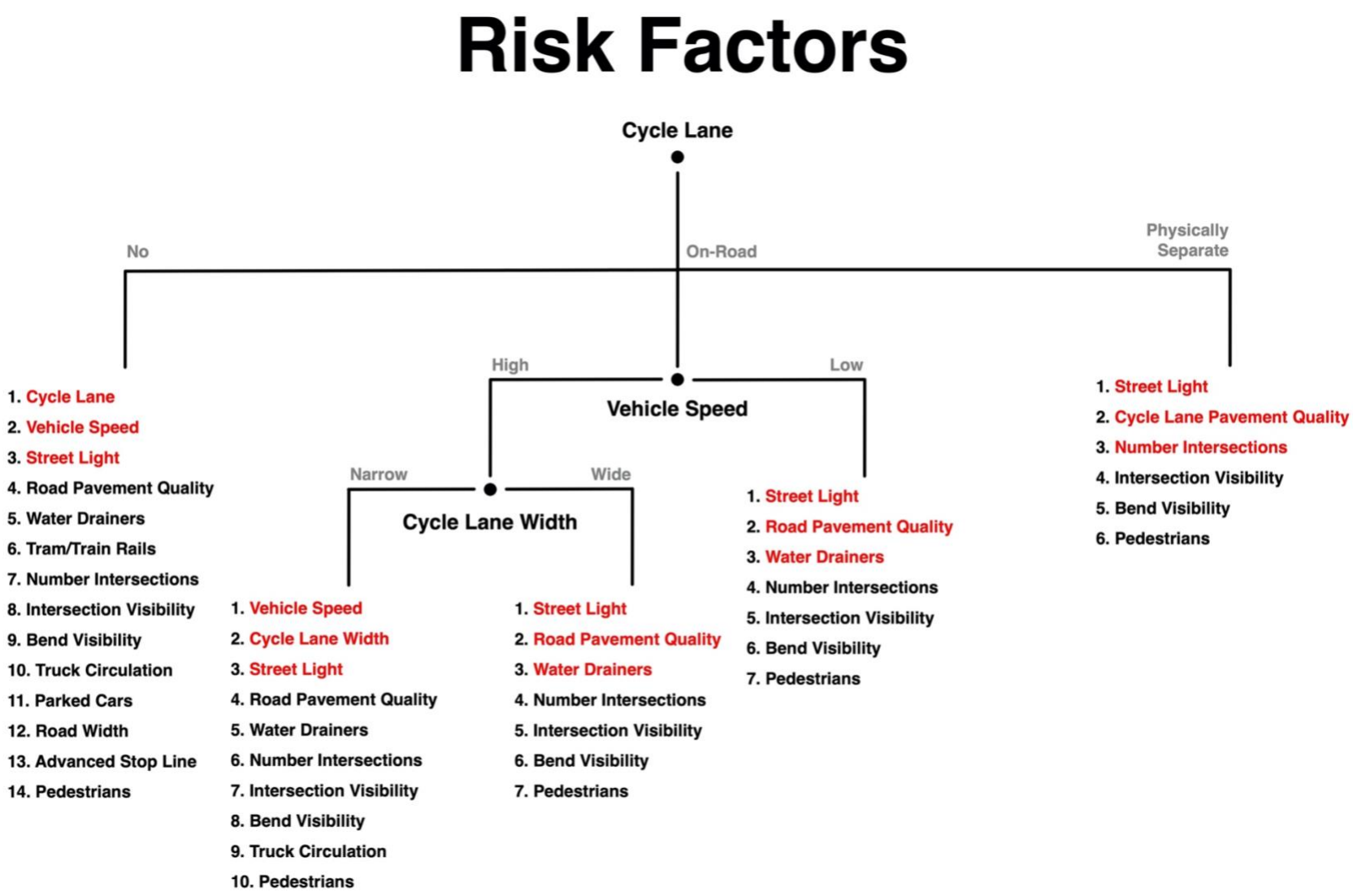

Figure 4 Identified cyclists' risk factors in 5 scenarios on the roads of London. Highlighted in red are the most relevant based on fatality and injury rates.

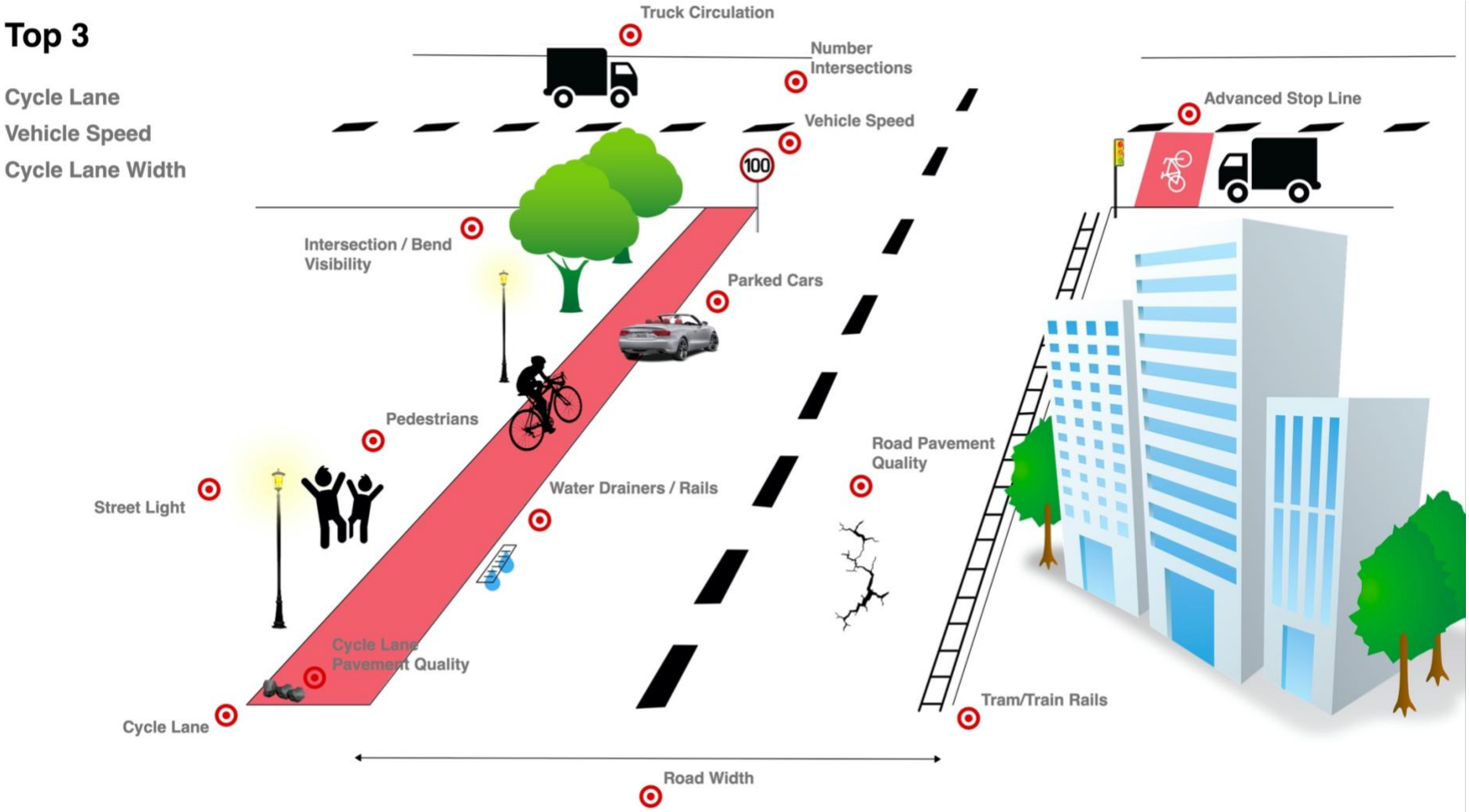

Figure 5 Cyclists' risk factors identified on the roads of London and depicted in a simulated scenario.

1.4. Training Datasets

Two object detection and two image/semantic segmentation training datasets were compared in terms of their discriminative power to identify cyclist's risk factors identified in Table _. Some were directly extracted from the Google Street View images of London, others were indirectly inferred. Features in Table _ with an asterisk are dynamic. Consequently, in the same location, they are expected to vary in number over time.

Below, four state-of-the-art datasets are compared before choosing the most suitable pre-trained deep learning models.

Table 2 Comparison between 4 of the biggest object detection and image segmentation datasets, with relevant data to assess road safety.

	Object Detection		Image Segmentation	
Risk Factor	MS Coco	Open Images V6	Cityscapes	ADE20K
Cycle Lane	-	-	Sidewalk*	-
Streetlight	-	Streetlight*	-	Streetlight* | Street Lamp*
Pedestrians (e.g.: children near schools)	People	Girl | Man | Person	Person	Person | Individual | Someone | Somebody | Mortal
Water Drainers	-	-	-	-
Tram/Train Rails	Train	Train	-	-
Number Intersections	-	-	Sidewalk* | Road	Sidewalk* | Pavement*
Intersections Visibility	-	-	Sidewalk* | Road	Sidewalk* | Pavement*
Bends Visibility	-	-	-	-
Vehicle Speed	Stop Sign* | Traffic Light*	Stop Sign* | Traffic Light* | Traffic Sign*	Traffic Light* | Traffic Sign*	Traffic Light* | Traffic Signal* | Stoplight*
Parked Cars	Car | Parking Meter*	Car | Taxi | Vehicle	Parking*	Car | Auto | Automobile | Machine | Motorcar
Lorries and other Large Vehicles	Bus | Train | Truck	Bus | Train | Van	Bus | Truck | On Rails | Caravan	Truck | Motortruck | Van
Road Width	-	-	Road*	Road* | Route*
Pavement Quality (Pits, Trenches, Tree Root Encroachments)	-	-	-	-
Advanced Stop Line	-	-	-	-

As mentioned above, some risk factors can be captured directly, while others require an indirect approach.

None of these datasets contains labelled cycle lanes. Although, Cityscapes is able to identify physically separated ones along with sidewalks, as part of the same category.

Open Images and ADE20K contain in their dataset the specific category of objects streetlight.

For the presence of pedestrians, all datasets contain various elements that let us infer about how crowded a given road might be.

None of the 4 datasets contain images with labels for features present on the ground. This include water drainers, rails, pavement quality or road lines (such as advanced stop line).

One way to indirectly capture tram rails would be to infer them by the presence of trams. Both MS Coco and Open Images datasets contain this element.

Number of intersections can be calculated by the number of interruptions in the sidewalk or the presence of perpendicular roads. Both situations can be captured using the image segmentation datasets.

Lack of visibility in intersections can be inferred by the presence of non 90 degrees road connections.

In terms of bend visibility, there are no clear elements in any of the 4 datasets that can be easily used to capture this.

Traffic calming signs are known to slowdown vehicle speed. Datasets contain labels to detect traffic lights, stop signs, stop lights and other traffic signs.

Parked cars to be detected looking for the presence of parking meters and parking areas delimited by the respective lines.

Lorries and large vehicles to be detected on the road. All datasets contain labels for these types of vehicles.

Finally, image segmentation will be used to calculate road width.

Microsoft Coco Dataset

Number of images:

Classes:

Cityscapes Dataset

Number of images:

Classes:

1.5. Object Detection

For the object detection, it will be used YOLOv5 pre-trained in the Coco dataset. This project uses static images to identify cyclist risk factors. In the future, this technique may allow us to use video sources instead and obtain more detail on the risk factor affecting cyclist's safety. This can be particularly relevant in the case of dynamic features like the ones included in Table _, with no asterisk.

1.5.1. YOLOv5

YOLOv5 is the most recent version of YOLO which was originally developed by Joseph Redmon. First version runs in framework called Darknet which was purposely built to execute YOLO.

Version 5 is the 2nd model which was not developed by Joseph Redmon (after version 4) and the first running in the state-of-the-art machine learning framework PyTorch.

This model was pre-trained using Coco dataset. Thus, it is able to identify 80 object categories. Distributed over 11 categories.

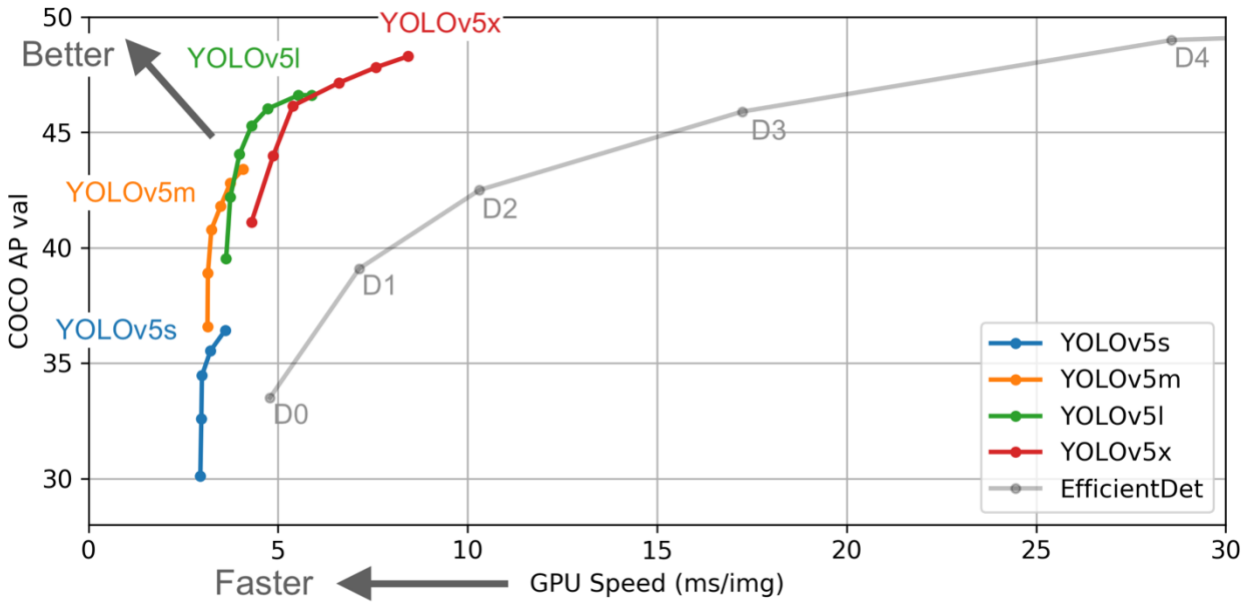

Figure 6 The most up to date YOLO model is the version 5 (July 2020). It was released with 4 different sets of weights of varying accuracy and storage requirements. All data from the project was obtained using YOLOv5x, the most accurate. The presence of EfficientDet highlights the speed of detection of YOLOv5, keeping the same high accuracy.

Table 3 Specifications for all sets of weights released with YOLOv5. Generally, as average precision increases, more processing power is required from the GPU to be executed.

Model	AP^{val}	AP^{test}	AP_{50}	$Speed_{GPU}$	FPS_{GPU}	Params	FLOPS	Weights Size (MB)
YOLOv5s	36.6	36.6	55.8	2.1	476	7.5M	13.2B	14
YOLOv5m	43.4	43.4	62.4	3.0	333	21.8M	39.4B	42
YOLOv5l	46.6	46.7	65.4	3.9	256	47.8M	88.1B	92
YOLOv5x	48.4	48.4	66.9	6.1	164	89.0M	166.4B	170
YOLOv3-SPP	45.6	45.5	65.2	4.5	222	63.0M	118.0B	241

1.6. Image Segmentation

Image segmentation will be performed using a pre-trained model with Cityscapes dataset. This method will not only allow to detect the presence of several objects in the images, but also to consider their sizes and shapes. Important factors to consider when trying to calculate road widths.

Image segmentation provides information not only on the presence of several structures (30 categories), but also their shape and location in the image. Once there are certain road safety factors that are enough to know about their absolute number of counts, such as vehicles, others importantly rely on their dimensions to tell whether they are beneficial or detrimental for cycling.

1.6.1. PSPNet101

Image segmentation models reached a precision plateau (in terms of average IoU) in the previous 2 years. Due to their long execution times, it was chosen the model executing faster and with the higher precision.

PSPNet101 was pre-trained in Cityscapes dataset. This way, it was able to label all pixels from an image across 100 categories.

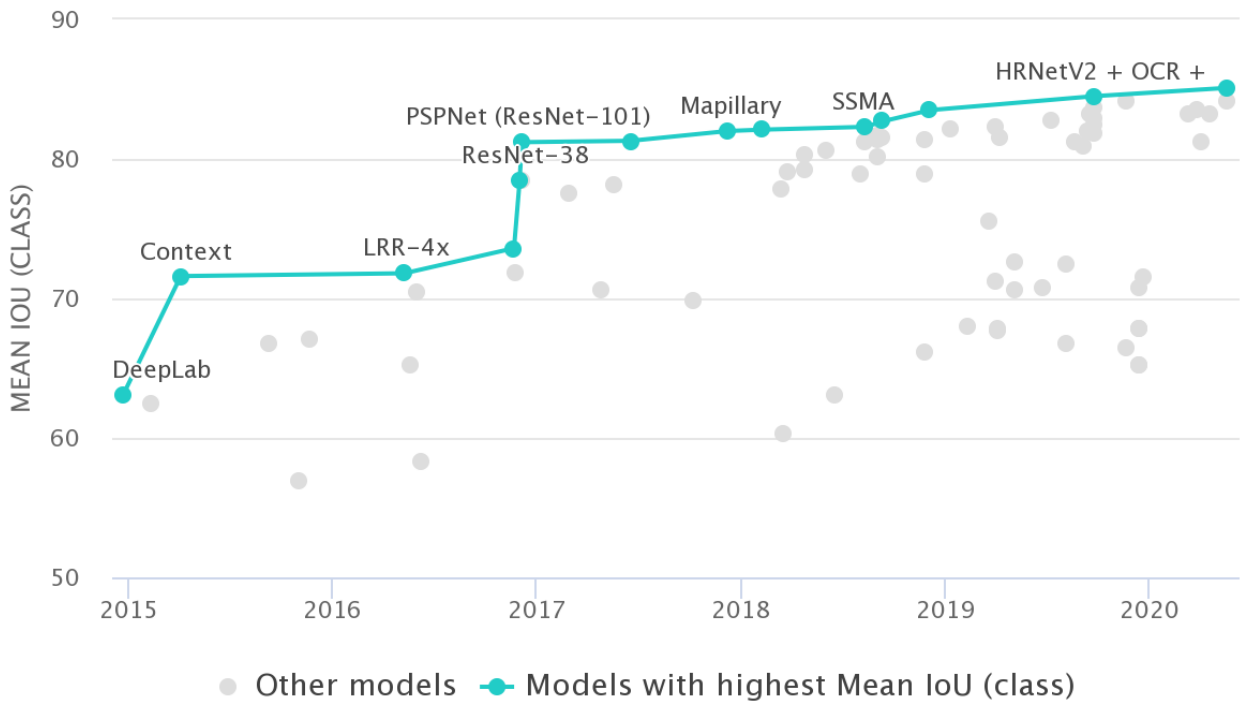

Figure 7 Evolution of image segmentation models over time. Since 2017, the increase in the mean IoU measure has been very small.

1.7. Objectives

2. Methodology

In this section it will be detailed how GSV imagery dataset was storage and processed using YOLOv5 and PSPNet101 models. The choice of the respective parameters. Plus, the software and hardware that was used to execute them. At the end, it is provided a roadmap of the project, since project's allocation, until the submission month.

2.1. GSV Imagery Dataset

There were multiple options to store GSV imagery dataset. Dropbox, Google Drive, Imperial RDS and locally were some of them.

GSV imagery dataset was obtained and pre-processed before the start of this project by Imperial's School of Public Health members. The full set of images is organized in datapoints. Each containing 4 perspectives covering 360 degrees angle. A separate file associates each to a given London area (OA, MSOA and LSOA).

Due to high storage requirements, all images used in this project were storage in Imperial facilities. Images in the Research Data Store were accessed using Globus platform.

2.2. YOLOv5

To execute YOLOv5, Imperial's High-Performance Computing cluster was used. It was accessed using the VPN connection tool – *Tunnelblick*.

Due to the speed of execution of YOLOv5, it was used one single P1000 GPU. And the set of weights handling the most accurate results was chosen- YOLOv5x. No job was submitted to HPC.

It was defined a minimum confidence of 0.5 for every detection. Higher than the standard value of 0.4. Only the text files containing the detected objects and respective locations were saved. An example is provided in Figure _. It includes numerical code for each object and the coordinate of the detection rectangle:

2 0.155469 0.675 0.210938 0.14375

2 0.517187 0.642969 0.1375 0.129688

2 0.774219 0.702344 0.348437 0.242188

2 0.138281 0.589063 0.126563 0.04375

2 0.25625 0.621094 0.08125 0.0703125

To test the efficacy of the model, it was saved and analysed one object detected image per LSOA across the full dataset. A total of 4832 images.

2.3. PSPNet101

Although it was already available a pre-liminary version of the implementation executing PSPNet101 (provided by Esra Suel), the modifications were made to overcome incompatibilities with the new version of TensorFlow. Moreover, originally it was used Python *multiprocessing* tool to accelerate the execution. At the end, splitting the original dataset in multiple batches and submitting them to HPC was the chosen procedure.

State-of-the-art image segmentation methods are significantly slower than object detection. For this reason, the dataset was splitted in 13 batches and executed parallelly in 13 P100 GPUs. This way, 13 jobs were submitted to the HPC. P100 was the chosen GPU due to its higher processing power when compared to the others available (Table _).

Table 4 GPU types available on the Imperial High-Performance Computing cluster. P100 was used in this project.

GPU Type	Single Precision (TFLOPS)	Double Precision (TFLOPS)	Memory (GB)	Memory Bandwidth (GB/s)
P1000	36.6	36.6	55.8	2.1
K80	43.4	43.4	62.4	3.0
P100	46.6	46.7	65.4	3.9
RTX6000	48.4	48.4	66.9	6.1

The output was the total number of images in GSV dataset segmented. Each pixel was coloured accordingly to the structure that was detected. After, two Python functions were implemented. One that generates a dictionary linking each RGB colour to a given object class. Another, that receives as input the full dataset of segmented images and outputs the total number of labelled pixels for each category.

Figure 8 NVIDIA P100. GPU used to detect objects and segment images from the GSV imagery dataset.

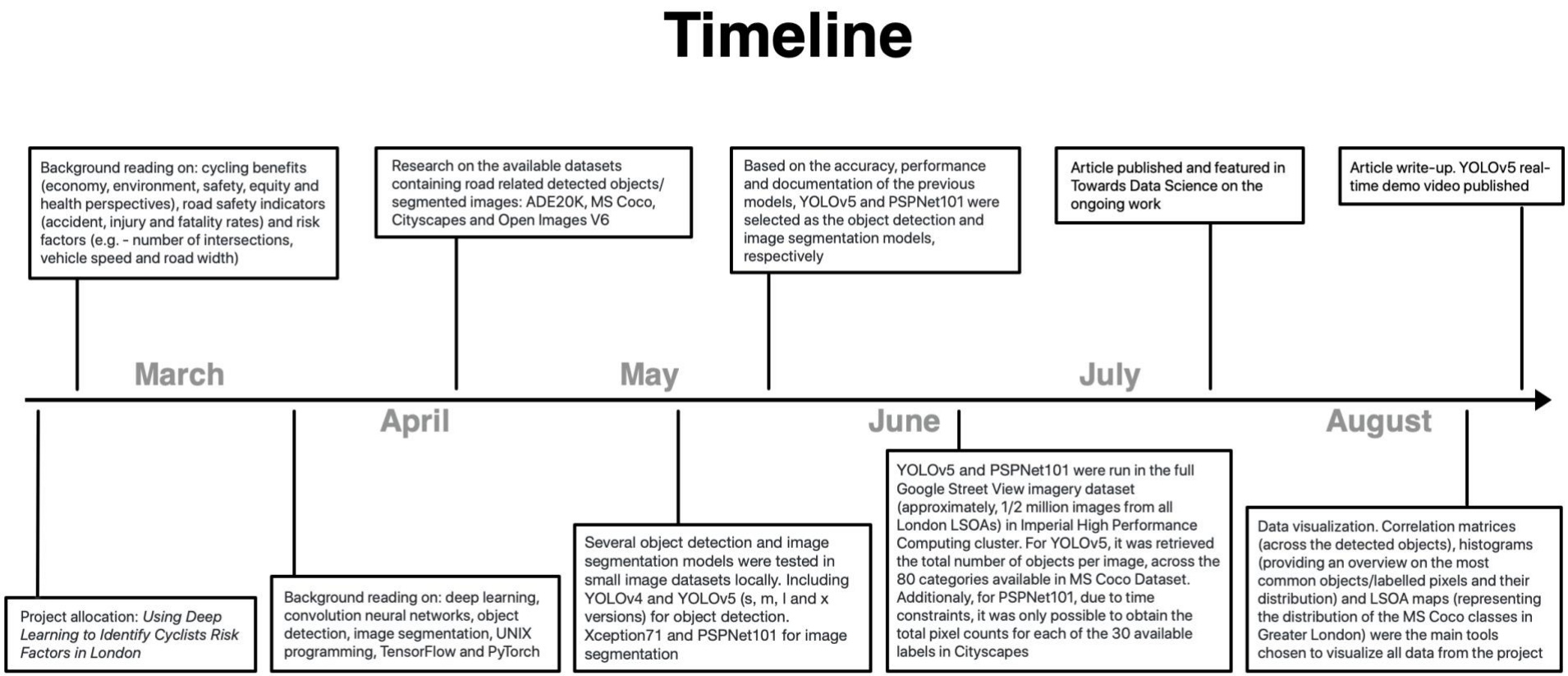

Figure 9 Project's roadmap since it started in March, until the submission month, August.

3. Results

In this section, the results are presented along with their discussion. First, it is provided an overview of the GSV imagery dataset distribution across all London LSOAs. Then, object detection and image segmentation outputs are introduced.

In the case of the first, the most detected objects are shown in relative and absolute numbers. After, a correlation matrix including the most common objects is described in terms of its most significative associations. Object distribution was also analysed at an LSOA level. Two extra LSOA maps were added as a step forward in generating a universal metric for assessing cyclist's road safety. After, the most common object misclassifications are presented. Finally, all the files used and generated in this section were displayed in a table.

For image segmentation, the relative and absolute number of pixels counts for each label were presented. Then,

3.1. GSV Dataset

GSV dataset contains a set of 518350 images which are spread across Greater London in 129588 points. For each datapoint there are 4 images available, ranging from 0 to 360 degrees.

They were also pre-processed to guarantee a maximum uniformity when analysing different image data points or angles.

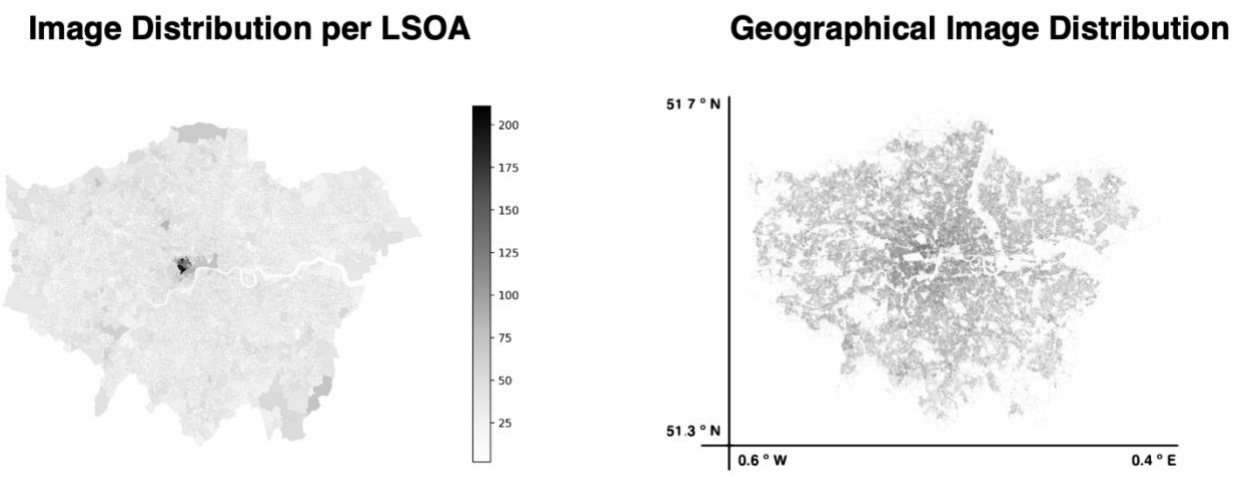

Figure 10 (Left) London LSOAs coloured accordingly to the number of available images in the GSV dataset. (Right) Geographical distribution (latitude and longitude) of the same set of images.

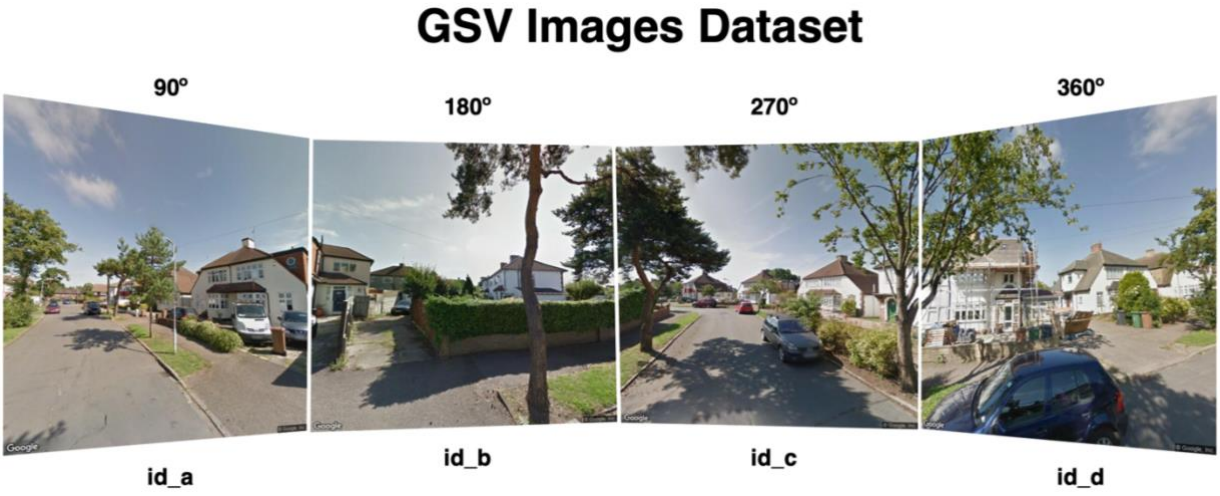

Figure 11 For each datapoint in Figure _, there are 4 images associated. Each one capture 90 degrees of the surroundings.

Table 5 Statistics on the availability of GSV images in the dataset, across all London LSOAs.

Minimum	Maximum	Mean	Standard Deviation	Mode	Median
1	211	27	24	25	11

Table 6 Not all images in the GSV dataset are LSOA identified. For this reason, a smaller set was used in the analysis.

N. Images GSV Dataset	N. LSOA Identified Images	N. Non-Repeated Identified Images	N. LSOA with Images
518350	512812	478724	24

3.1.1. Files

All GSV raw images analysis was performed in a Jupyter Notebook. Processed data and implemented functions were made publicly available in the project's GitHub repository. Table _ compiles all the generated files.

Available in the project's GitHub repository are a dictionary file converting GSV image IDs into the London LSOAs they belong. And a second linking each LSOA to the number of GSV images available (Table 7).

Table 7 GSV generated files used to normalize objects distribution across each LSOA in London

File	Description
imgId_lsoa.json	File converting GSV image ids into the London LSOAs they belong
lsoa_number_images.json	Number of GSV images for each London LSOA
road_safety.ipynb	Project's Jupyter notebook where all data analysis was done

3.2. Object Detection | YOLOv5

An example of an image after running YOLOv5x is provided in Figure _. All cars, trucks and people in the image were accurately detected. Although it is not significative analysing the accuracy of a model based on a single image, all the 10 images processed in Figure _, plus the 4832 made available across all London LSOAs show the accuracy of the most common objects in the Coco training dataset to be closer to be very high.

Figure 12 Example of a GSV image after executing YOLOv5x. Detection of a car reflection in one of the windows demonstrates the power to capture the smallest details.

Next, the relative and absolute distributions of all objects in the London imagery is presented.

3.2.1. Dataset Objects Distribution

Relative distribution of the top 15 most detected categories of objects were plotted in Figure _.

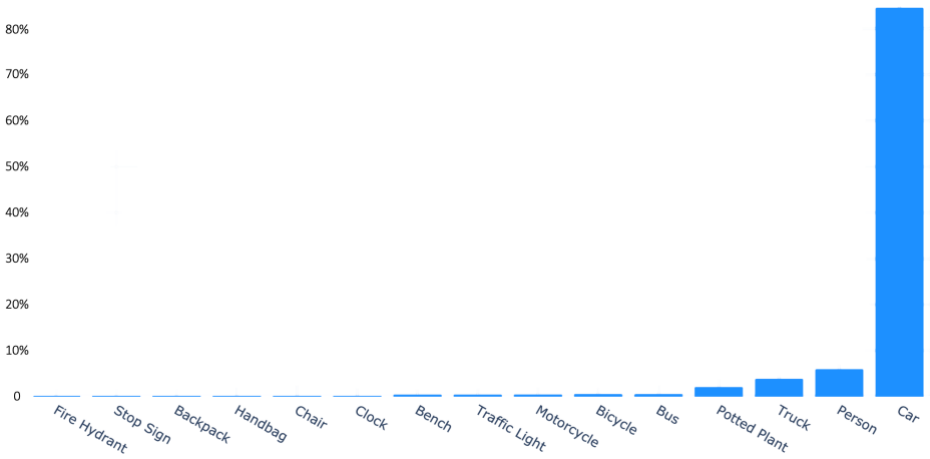

Figure 13 Relative distribution of top 15 detected objects across all London LSOAs.

Once the dataset exclusively contains street view images, it was not expected to detect a big fraction of cars.

London is a city with a high populational density. For this reason, detecting people

Table 8 Absolute counting for top 15 most common detected objects.

Object	Number Detections	Object	Number Detections	Object	Number Detections
Car	2M	Bicycle	11K	Chair	2K
Person	107K	Motorcycle	9K	Handbag	2K
Truck	70K	Traffic Light	6K	Backpack	2K
Potted Plant	38K	Bench	5K	Stop Sign	1K
Bus	12K	Clock	3K	Fire Hydrant	1K

3.2.2. Correlation Matrix

After determining the most detected objects in the GSV dataset, it was studied the frequency they appear together. Using Pandas dataframe function *corr*, it was obtained the correlation matrix in Figure _.

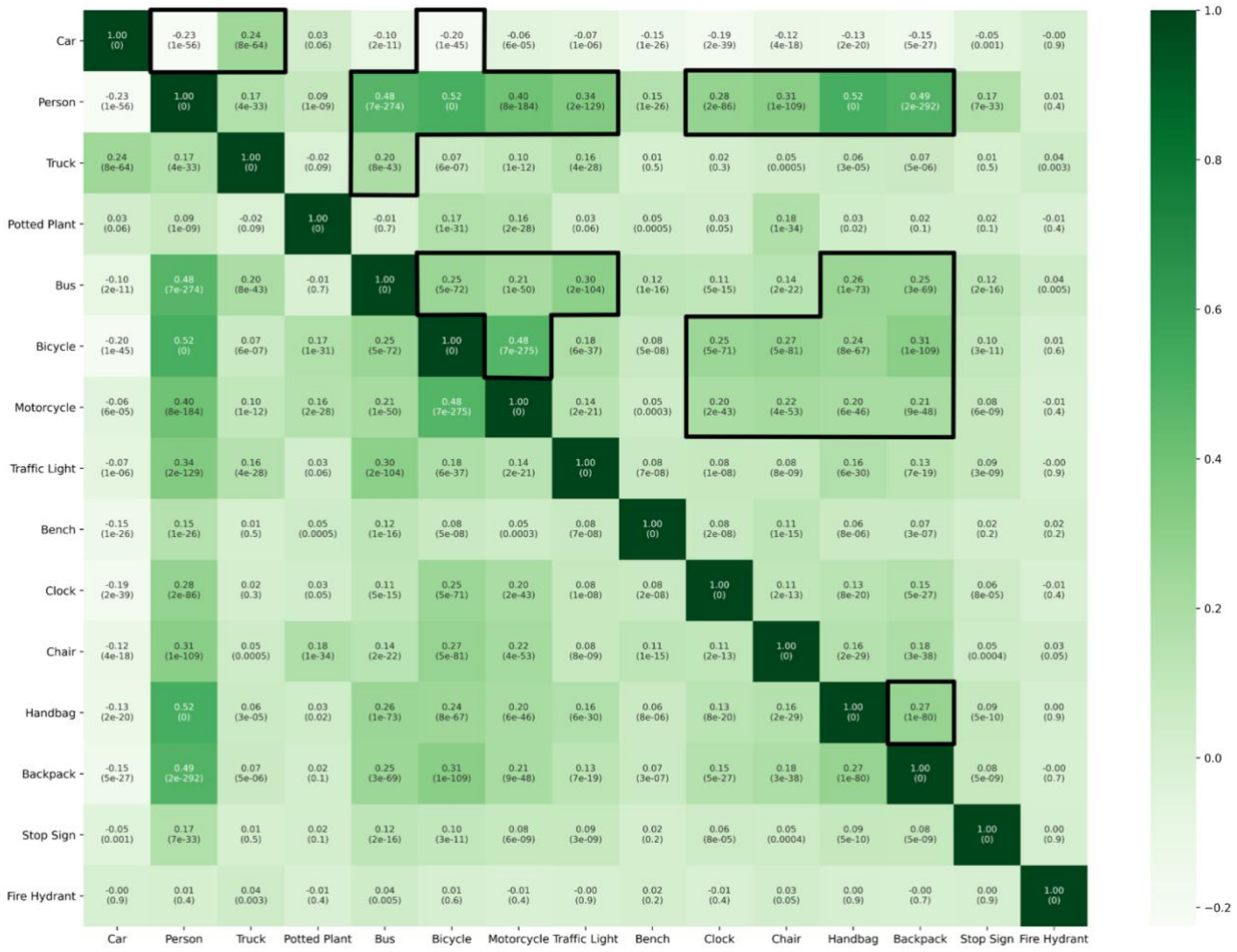

Figure 14 Top 15 detected objects correlation matrix. Inside each cell, on the top, it is Pearson correlation coefficient. On the bottom, the associated p-value.

After thresholding our analysis to correlations higher or lower than 0.2 or -0.2, respectively, and to the top 15 more common objects, it was verified the object with the highest number was *Person*. It strongly correlates with Bicycle and Handbags. Intuitively, this agrees with one would expect.

Inversely correlated in the matrix are *Car* with *Person* and *Bicycle*. This suggest that areas with high concentration of cars are dissuasive to cycling and walking.

3.2.3. LSOA Maps

Compiled in Figure _ were all the LSOA distributions determined important after reviewing cyclists' road safety literature and accounting for the available dataset categories.

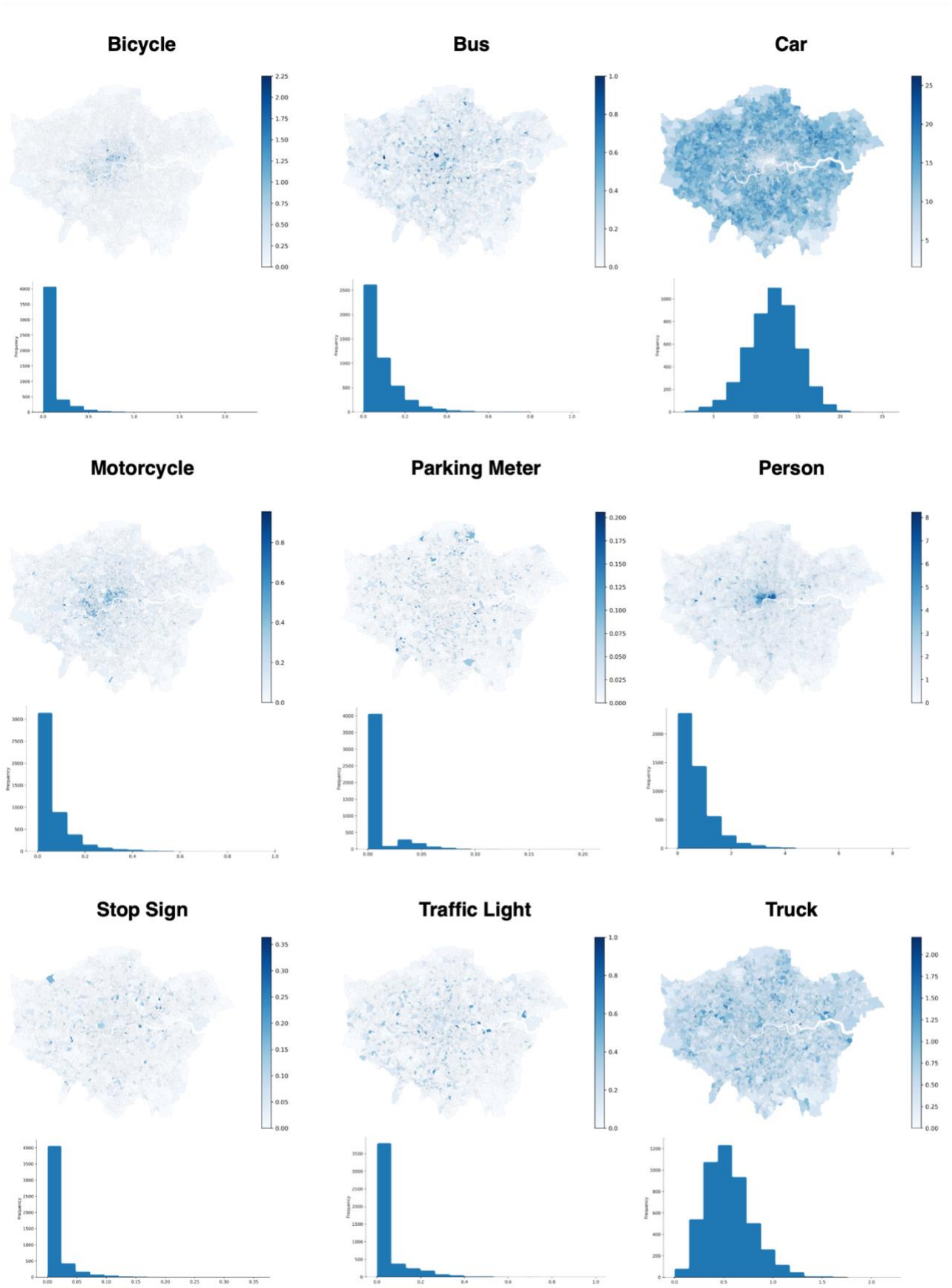

Figure 15 Detected objects' distribution across all London LSOAs. Plus, respective distribution histograms on the bottom of each atlas.

While reviewing the literature in cyclists' road safety, heavy vehicles were accounted responsible for high fatality rates. For this reason, the distribution of buses and trucks was included in the list. Crashes with cars are responsible by most cyclists' injuries and deaths. Traffic calming factors such as stop signs and traffic lights slow down road speed. Being speed one of the most important risk factors, the distribution of these objects was also studied. The presence of parking meters is known to be linked with parked cars, another factor contributing negatively for cycling safety. Presence of cyclists is known to raise awareness of other drivers, thus positively influences safety. Presence of people is inversely correlated with the presence of cars. Consequently, this is an additional positive factor. Although it is not clear the impact of motorcycles in cycling safety, they were included so that a plot of the traffic in London could be generated next.

Most bicycles were detected in Central London. Once this is a type of transport for short distances, they were essentially found in this area.

3.2.4. Traffic

It was not found a precise metric for cyclist's road safety based on the detected objects on the streets of London. Although, based on the set of LSOAs in Figure _, it was generated two extra ones that can represent a step forward in assessing road safety, not at a road level, but at an LSOA level.

One of the features that influences cyclist's safety is the number of other cyclists in the proximity. This happens because drivers are more aware on their presence. Moreover, the vast majority of serious injurious are caused by crashed between vehicles and cyclists. It was found there is a statistically significant negative correlation between the presence of cars and people. This way, the higher the presence of pedestrians, the lower the number of cars. Consequently, less risky for cyclist to get severely injured. *Bicycle* and *Person* LSOAs were combined in a single one, after summing the average number of each of these objects per image.

If cars are the main contributors for serious injuries, the counting of heavy vehicles is particularly relevant when assessing the fatality rates of a certain area. A second LSOA map was created joining the average counting per image of the following objects: *Bus*, *Car* and *Truck*.

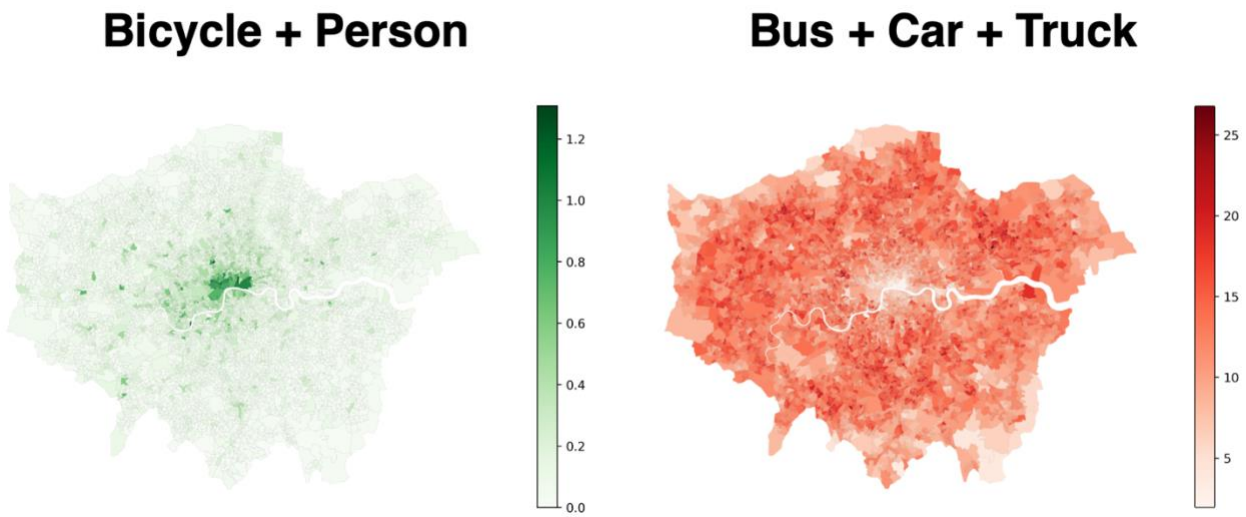

Figure 16 (Left) *Bicycle* and *Person* LSOA distributions were combined into a metric reflecting a positive score for cyclists' safety. (Right) *Bus*, *Car* and *Truck* distributions combined into a final atlas showing the traffic in London. This is inversely correlated with cyclists' safety.

3.2.5. Misclassifications

After individually analysing one YOLOv5 output image per LSOA for the complete London imagery dataset, it was found high levels of confidence to the top 15 most common object (Table _). The only exception being the clock detections. Moreover, YOLOv5 appears to be able to detect accurately any size of the most common objects in MS Coco training dataset. Even when partially occluded, the algorithm performs acceptably well. Despite rarely happening, the most unexpected observations were when the algorithm detected glass reflections of objects present on the roads of London. This demonstrates that even objects with very poor contrast were part of the set of detections.

It was compiled below a set of ten object detected images, so that the reader can verify by itself the accuracy of the algorithm. A link to the online folder containing the full set of 4832 object detected images is available in Table _.

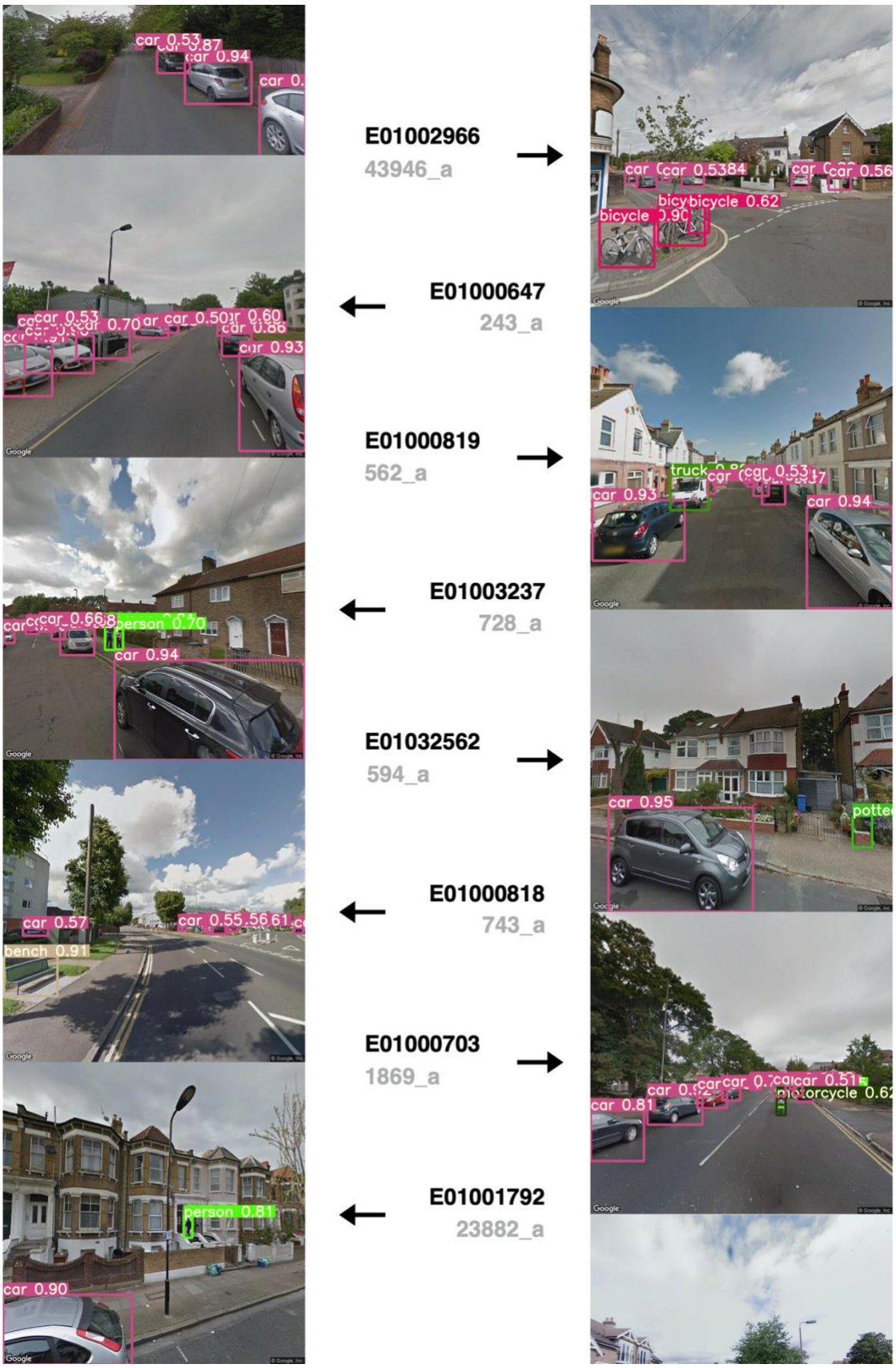

Figure 17 A glimpse on a short set of randomly picked object detected images from different LSOAs shows very few objects in MS Coco dataset categories were not detected.

3.2.6. Files

All object detection analysis was performed in a Jupyter Notebook. Processed data and implemented functions were made publicly available in the project's GitHub repository. Table _ compiles all the generated files.

Table 9 All files generated after running YOLOv5 in the GSV imagery dataset.

File	Description
total_stats.json	Number of objects detected by YOLOv5 in GSV imagery by class
Lsoa_objects_number.json	Number of objects detected by YOLOv5 in GSV imagery by class and LSOA
lsoa_objects_number_average_per_image.json	Average number of objects detected by YOLOv5 in GSV imagery per image (includes all classes and LSOAs). JSON format.
lsoa_objects_number_average_per_image.csv	Average number of objects detected by YOLOv5 in GSV imagery per image (includes all classes and LSOAs). CSV format
yolov5_lsoa	Folder with 1 processed image per LSOA
road_safety.ipynb	Project's Jupyter notebook where all data analysis was done

3.3. Image Segmentation | PSPNet101

All images from GSV imagery dataset were segmented. An example of a segmented image is provided in Figure _. It was identified with the respective label all the detected structures.

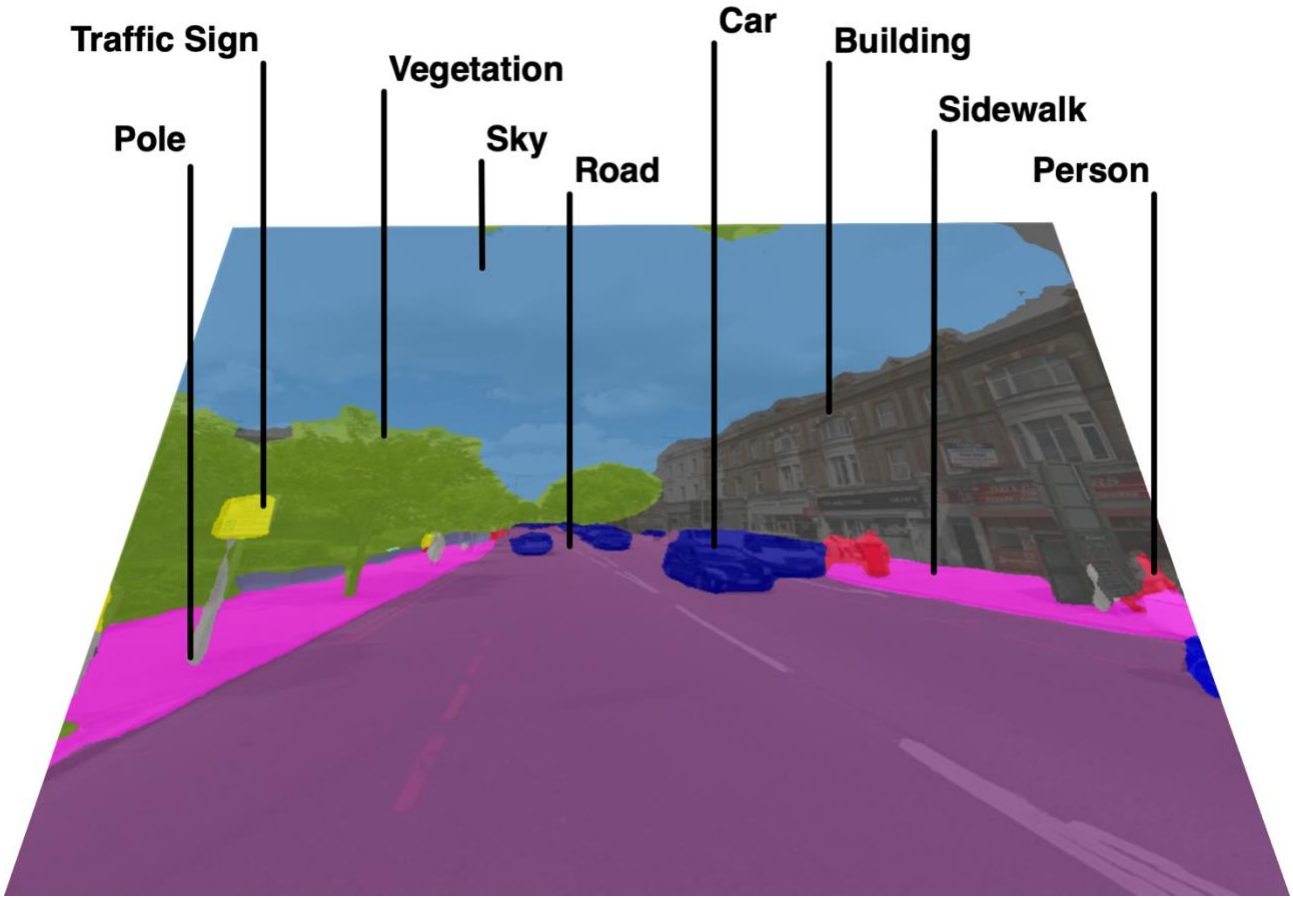

Figure 18 GSV image after segmentation using PSPNet101. All pixel labels present were identified.

It was obtained the relative and absolute distribution of pixels for all images in the GSV dataset. Buildings, sky, road, vegetation and cars cover more than 90% of the total area of complete GSV imagery dataset. In the case of the first 4 structures, this is explained by their intrinsic dimensions. Once this dataset exclusively contains images obtained from the roads of London, it was not unexpected finding a much higher number of cars than other objects. Finding a high number of car pixels is associated not with their size, but the frequency they appear in the images. This way, both object detection and image segmentation seem to be in accordance.

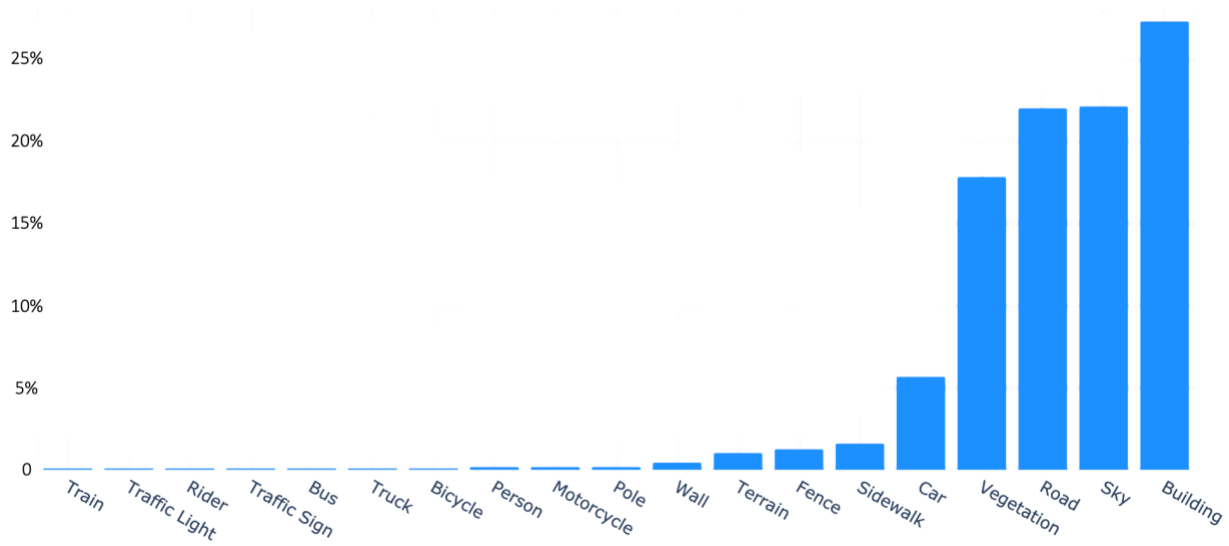

Figure 19 Relative distribution of labelled pixels after executing PSPNet101 in GSV imagery dataset.

Table 10 Absolute number of labelled pixels detected across all imagery dataset.

Label	Number Pixels	Label	Number Pixels	Label	Number Pixels	Label	Number Pixels
Building	47B	Sidewalk	3B	Motorcycle	299M	Traffic Sign	58M
Sky	38B	Fence	2B	Person	232M	Rider	14M
Road	38B	Terrain	2B	Bicycle	95M	Traffic Light	12M
Vegetation	30B	Wall	766M	Truck	91M	Train	7M
Car	10B	Pole	303M	Bus	81M		

The relative distribution of segmented pixels across the different categories also suggests that not only objects present on the roads were detected, but also in the surroundings, namely, in buildings and in the sky. Embedded on the buildings landscape, 2750 clocks were wrongly detected instead of satellite dishes. In the same area, 37917 potted plants were identified. In the sky, 234 airplanes were detected. Having detected a significant number of pixels labelled as sidewalk suggests objects regularly present are likely to be captured (107266 people were found, along with 5013 benches and 1168 fire hydrants).

Again, from an image segmentation point of view, GSV imagery dataset appears to be useful to estimate the area of roads and sidewalks due to the relative high number of pixels detected. The same applies to streetlights.

In spite only 303M pixels were identified, the dimensions of this object suggest that a significant number of those should have been detected.

After individually analysing 1 segmented image per LSOA for the complete dataset, it appears that both the area and shape of the roads and sidewalks can be accurately retrieved.

As it was identified in the Introduction, these last properties are relevant in a road safety context because they allow to calculate road and sidewalk width. And the presence of streetlights or poles as they are called in Cityscapes, it is a proxy to assess road visibility.

In Figure _, these concepts are exemplified along with an illustrative image on the side.

Image Segmentation

PSPNet101

Road

Road width is determinant for cyclists' safety.
In the presence of a shared cycling lane, this is crucial. Keeping a safe lateral distance between vehicles and cyclists (generally, legally enforced >1.5 m) decreases fatality rate of the latter.

Pole

Light conditions influence drivers and cyclists reaction time. In high speed roads, it tends to be very short. Cyclists are more aware on the presence of pedestrians during the night when there are streetlights.

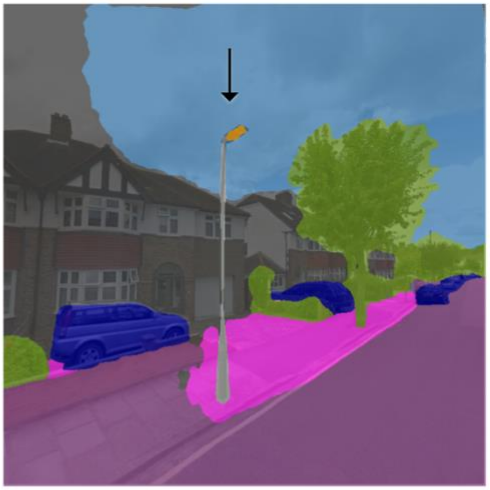

Sidewalk

Cityscapes incudes in this same category walking paths and physically separate cycling lanes.
The width of cycling lanes is one main factor contributing to cyclists safety. Allowing them to keep their distance from other vehicles and avoiding holes or other obstacles on the floor.

3.3.1. Misclassifications

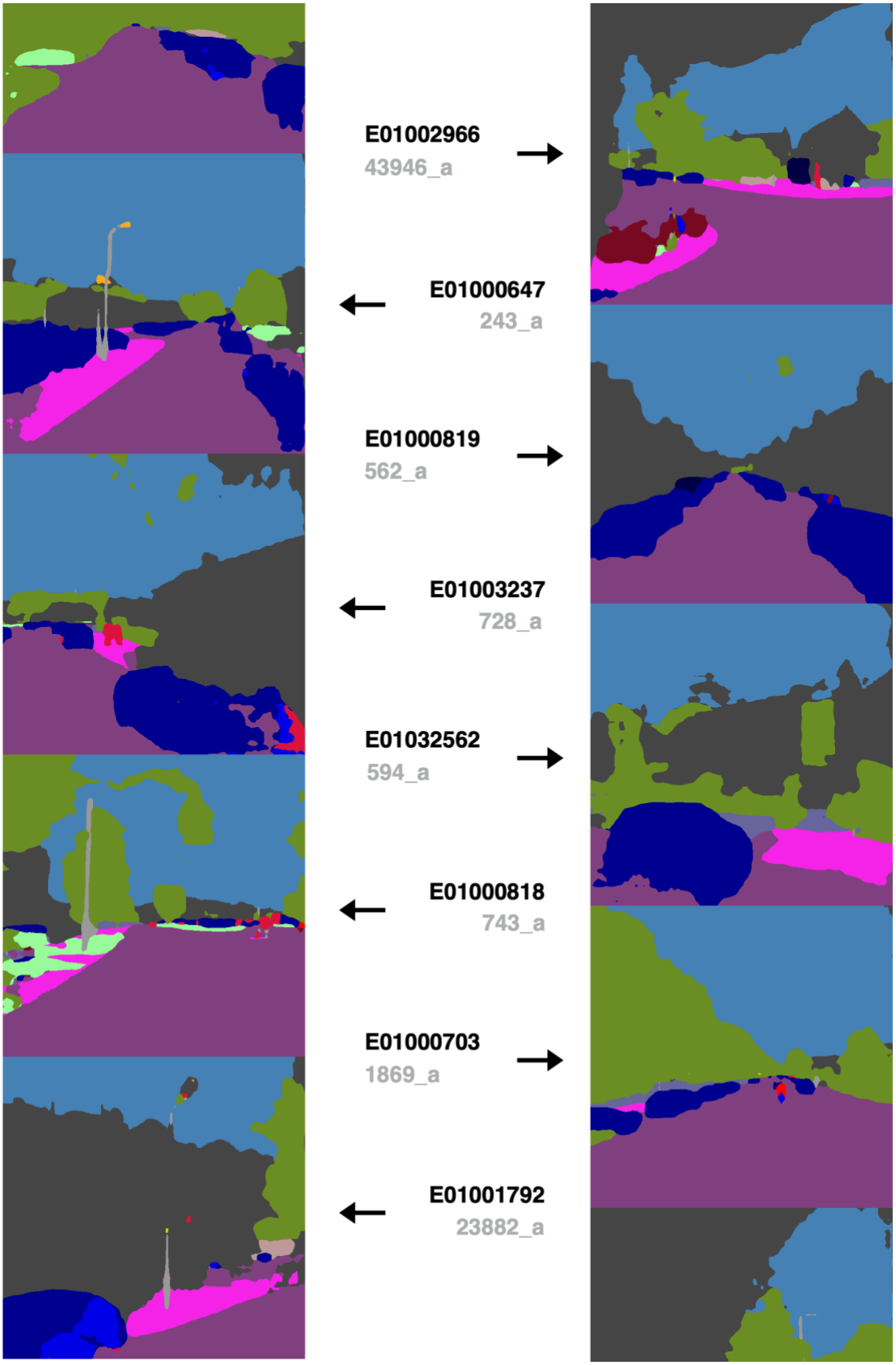

Figure 20 A glimpse on a short set of randomly segmented images from different LSOAs shows how important is to account for structure occlusion while capturing sizes and shapes.

3.3.2. Files

All image segmentation analysis was performed in a Jupyter Notebook. Processed data and implemented functions were made publicly available in the project's GitHub repository. Table _ compiles all the generated files.

Table 11 Generated files after executing PSPNet101 in London imagery.

File	Description
total_stats.json	Total number of pixels for each Cityscapes label in the GSV dataset
rgb_label.json	Conversion from RGB values to the respective cityscapes label
pspnet101_lsoa	Folder with 1 segmented image per LSOA
road_safety.ipynb	Project's Jupyter notebook where all data analysis was done

3.3.3. Future Directions

Due to time constraints, it was not possible to present a detailed image segmentation analysis, similarly to the previous object detection section. Nevertheless, below are some approaches we considered during this project.

There are objects in the streets of London that were not identified using YOLOv5 due to limitations of the dataset (MS Coco) that was used to train the model. Moreover, for some, it might be also useful to account to their shapes.

It is possible to extract the number of streetlight lamps and their locations for the GSV imagery dataset. Although there is not a specific category for those, most of the identified *Pole* and *Polegroup* were light sources. This was concluded after analysing one image for all London LSOAs. In terms of image resolution, it may not be enough to capture streetlights poles, depending on the distance the image was captured. This appears to be a problem only in the case one pretends to retrieve their shape.

Another structure that was identified as determinant for cyclist's road safety was the presence of cycle lanes. It was not possible to identify a one dataset with segmented images with specific labels for these lanes.

Consequently, there were no pre-trained models. Cityscapes considers them part of the road when those are shared with other vehicles. Or, sidewalk, when they are physically separate. Although we did not find evidence whether sidewalks correlate with cyclist's safety, in the future, proven there is an important association, PSPNet101 pre-trained in Cityscapes will allow us to extract this information. Two of the main drawbacks of detecting sidewalks are the angle of the analysed image and obstructing structures such as *Vegetation*, *Person* or other common objects.

Road width was identified to be crucial for cyclist's safety, mainly when there is no physical separation between vehicles and the cycle lane, and in high speed roads. Estimating road width is not a straightforward task due to the angle the image was captured and presence of obstructive objects.

Due to time constraints,

Figure _ summarizes all information extractable by PSPNet101 using GSV imagery dataset that was found to be determinant to asses road safety in a cyclist's perspective.

4. Conclusion

5. Appendices

5.1. Detected Objects

One of the main goals of this project was to show the potential of Street View imagery. Given a dataset big enough, there are plenty of information that can be extracted.

While analyzing all the processed LSOAs atlas, it was found two that illustrate the potential of this technique: *Airplane* and *Potted Plant* categories.

In the case of the first, it was detected a higher density of planes per image in the areas next to the airports of Heathrow and City of London. Moreover, all detected planes are on the right of each of these structures. This phenomenon is explained by the wind direction West-> East, which makes the planes preferably landing from East-> West. Thus, only images taken on the right contain them. Finally, it is also clear the difference on the number of detections next to each of these airports. Due to the increased air traffic of Heathrow, most of them are located in its proximities.

Potted plants were also frequently detected. These were mainly present in images closer to the biggest parks of London. This category includes all vegetation inserted in any type of pot. Given vegetation was the second most labeled type of pixels across the GSV dataset after executing PSPNet101, it is not surprising the high levels of captured potted plants (fourth most detected object).

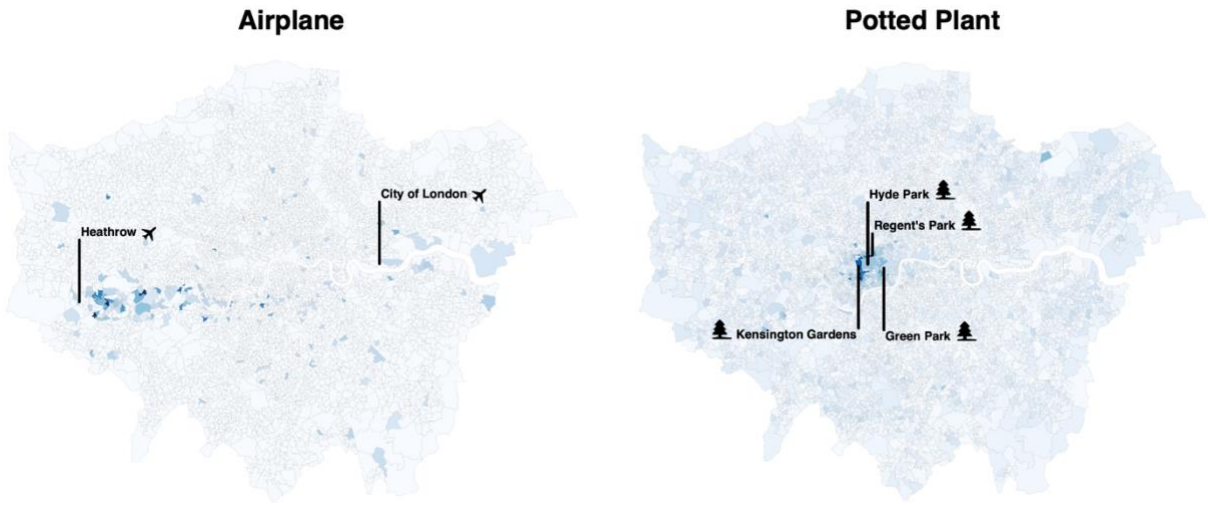

Figure 21 (Left) Density of planes present in images taken next to the closest London airports is in agreement with what was expected to observe. (Right) Identically, the biggest density of potted plants was observed closer to the biggest parks.

5.2. Misclassifications

For the objects we defined as relevant to cyclist's road safety, the number of misclassifications was very small. This was achieved because it was defined a high threshold of 0.5 to count as a detection and in MS Coco training dataset the most common objects are the ones we are interested.

Although, there were objects consistently misclassified. The most common were satellite dishes being detected as clocks. Depending on the angle, arm dishes can easily resemble a clock pointer. It was detected 2750 clocks in the complete GSV imagery dataset (Figure _). Other less represented objects were also wrongly identified. Sometimes due to their shape, others because of their texture. Another example of the former were the detection of boats instead of construction containers or, for the latter, benches instead of fences.

Figure 22 The most common misclassification identified after executing YOLOv5 was the detection of clocks instead of satellite dishes.

References

[1] H. Arem and E. Loftfield, “Cancer Epidemiology: A Survey of Modifiable Risk Factors for Prevention and Survivorship,” *American Journal of Lifestyle Medicine,* vol. 12, no. 3, p. 200–210, 2018.

[2] M. S. Donaldson, “Nutrition and cancer,” *Nutrition Journal,* vol. 3, pp. 19-25, 2004.

[3] M. Jovanovik, A. Bogojeska and D. e. a. Trajanov, “Inferring Cuisine - Drug Interactions Using the Linked Data Approach,” *Scientific Reports,* vol. 5, no. 9346, 2015.

[4] K. Veselkov, G. Gonzalez, S. Aljifri, D. Galea, R. Mirnezami, J. Youssef, M. Bronstein and I. Laponogov, “HyperFoods: Machine intelligent mapping of cancer-beating molecules in foods,” *Scientific Reports,* vol. 3, no. 9237, 2019.

[5] C. Anderson, “A survey of food recommenders,” *ArXiv,* vol. abs/1809.02862, 2018.

[6] “pedbikeinfo,” Pedestrian and Bicycle Information Center, [Online]. Available: http://www.pedbikeinfo.org/. [Accessed 19 April 2020].

[7] E. R. S. Observatory, “Traffic Safety Basic Facts 2018,” European Commission, 2018.

[8] P. A. a. O. CDC (Division of Nutrition, “Physical Activity,” 4 February 2019. [Online]. Available: https://www.cdc.gov/physicalactivity/about-physical-activity/pdfs/healthy-strong-america-201902_508.pdf. [Accessed 19 April 2020].

[9] “Factsheet: Cyclist safety,” European Commission, [Online]. Available: https://ec.europa.eu/transport/sites/transport/files/themes/urban/doc/cyclist_safety_onepager.pdf. [Accessed 8 April 2020].

[10] “Bicycle Facilities,” iRAP, [Online]. Available: http://toolkit.irap.org/default.asp?page=treatment&id=1. [Accessed 8 April 2020].

[11] “Bike rider safety,” Victorian Transport Resources, [Online]. Available: https://www.vicroads.vic.gov.au/safety-and-road-rules/cyclist-safety/bike-rider-safety. [Accessed 8 April 2020].

[12] “Road Safety Commission,” Government of Western Australia, [Online]. Available: https://www.rsc.wa.gov.au/RSC/media/Documents/Resources/Cyclists-INFO-SHEET.pdf. [Accessed 8 April 2020].

[13] “Driving & cycling safety,” Transport for London, [Online]. Available: https://tfl.gov.uk/travel-information/safety/road-safety-advice/driving-and-cycling-safety. [Accessed 8 April 2020].

[14] “Bicycle Safety,” National Highway Traffic Safety Administration, [Online]. Available: https://www.nhtsa.gov/road-safety/bicycle-safety. [Accessed 8 April 2020].

[15] SafetyNet, “Pedestrians & Cyclists,” 2009. [Online]. Available: https://ec.europa.eu/transport/road_safety/sites/roadsafety/files/specialist/knowledge/pdf/pedestrians.pdf. [Accessed 13 May 2020].

[16] K. T. e. al, “Route Infrastructure and the Risk of Injuries to Bicyclists: A Case-Crossover Study,” *American Journal of Public Health,* vol. 102, no. 12, pp. 2336-2343, 2012.

[17] L. Chen, C. Chen, R. Srinivasan, C. E. McKnight, R. Ewing and M. Roe, “Evaluating the Safety Effects of Bicycle Lanes in New York City,” *American Journal of Public Health,* vol. 102, no. 6, p. 1120–1127, 2012.

[18] “Cycling - preventing injury,” Victoria State Government, November 2013. [Online]. Available: https://www.betterhealth.vic.gov.au/health/HealthyLiving/cycling-preventing-injury. [Accessed 7 May 2020].

[19] “Speed and accident risk,” European Commission, 8 May 2020. [Online]. Available: https://ec.europa.eu/transport/road_safety/specialist/knowledge/speed/speed_is_a_central_issue_in_road_safety/speed_and_accident_risk_en. [Accessed 8 May 2020].

[20] “What forces can be tolerated the human body?,” European Commission, Mobility and Transport, 9 May 2020. [Online]. Available: https://ec.europa.eu/transport/road_safety/specialist/knowledge/vehicle/key_issues_for_vehicle_safety_design/what_forces_can_be_tolerated_the_human_body_en. [Accessed 9 May 2020].

[21] C. a. H. N. Tingvall, "Vision Zero - An ethical approach to safety and mobility," in *6th ITE International Conference Road Safety & Traffic Enforcement: Beyond 2000*, Melbourne, 1999.

[22] E. Pasanen, "Driving speeds and pedestrian safety," 1991.

[23] S. M. G. Ashton, "Benefits from changes in vehicle exterior design," in *Proceedings of the Society of Automotive Engineers*, Detroit, MI, 1983.

[24] V. S. M. R. e. a. Asgarzadeh M, "The role of intersection and street design on severity of bicycle-motor vehicle crashes," *Injury Prevention,* vol. 23, pp. 179-185, 2017.

[25] L. Dablanc, "Goods transport in large European cities: Difficult to organize, difficult to modernize," *Transportation Research Part A: Policy and Practice,* vol. 41, no. 3, p. 280–285, 2007.

[26] M. Jaller, J. Holguín-Veras and S. Hodge, "Parking in the city: Challenges for freight traffic," *Transportation Research Record: Journal of Transportation Research Board,* vol. 2379, p. 46–56, 2013.

[27] A. Conway, N. Tavernier, V. Leal-Tavares, N. Gharamani, L. Chauvet, M. Chiu and X. Bing Yeap, "Freight in a bicycle-friendly city," *Transportation Research Record: Journal of Transportation Research Board,* vol. 2547, p. 91–101, 2016.

[28] J.-K. Kim, S. Kim, G. F. Ulfarsson and L. Porrello, "Bicyclist injury severities in bicycle-motor vehicle accidents," *Accident Analysis & Prevention,* vol. 39, no. 2, p. 238–251, 2007.

[29] J. Manson, S. Cooper, A. West, E. Foster, E. Cole and N. R. M. Tai, "Major trauma and urban cyclists: physiological status and injury profile," *Emergency Medicine Journal,* vol. 30, no. 1, p. 32–37, 2012.

[30] S. Kaplan, K. Vavatsoulas and C. G. Prato, "Aggravating and mitigating factors associated with cyclist injury severity in Denmark," *Journal of Safety Research,* vol. 50, p. 75–82, 2014.

[31] P. Chen and Q. Shen, "Built environment effects on cyclist injury severity in automobile-involved bicycle crashes," *Accident Analysis & Prevention,* vol. 86, p. 239–246, 2016.

[32] P. e. al., "Transportation Research Procedia," vol. 25, p. 999–1007, 2017.

[33] M. McCarthy and K. Gilbert, "Cyclist road deaths in London 1985–1992: Drivers, vehicles, manoeuvres and injuries," *Accident Analysis & Prevention,* vol. 28, no. 2, p. 275–279, 1996.

[34] A. S. Morgan, H. B. Dale, W. E. Lee and P. J. Edwards, “Deaths of cyclists in London: Trends from 1992 to 2006,” *BMC Public Health,* vol. 10, no. 669, p. 1–5, 2010.

[35] P. Tuckela, W. Milczarskib and R. Maiselc, “Pedestrian injuries due to collisions with bicycles in New York and California,” *Journal of Safety Research,* vol. 51, pp. 7-13, 2014.

[36] D. Dufour, “European Commission - Intelligent Energy Europe,” February 2010. [Online]. Available: https://ec.europa.eu/energy/intelligent/projects/sites/iee-projects/files/projects/documents/presto_fact_sheet_cyclists_and_pedestrians_en.pdf. [Accessed 11 May 2020].

[37] J. Marin, A. Biswas, F. Ofli, N. Hynes, A. Salvador, Y. Aytar, I. Weber and A. Torralba, “Recipe1M+: A Dataset for Learning Cross-Modal Embeddings for Cooking Recipes and Food Images,” *IEEE Transactions on Pattern Analysis and Machine Intelligence,* 2019.

[38] R. A. Ferdman, “Map: The Countries That Drink the Most Tea,” The Atlantic, 21 January 2014. [Online]. Available: https://www.theatlantic.com/international/archive/2014/01/map-the-countries-that-drink-the-most-tea/283231/. [Accessed 7 March 2020].

[39] “Mapchart,” [Online]. Available: https://mapchart.net/world.html. [Accessed 7 March 2020].

[40] A. Maruca, R. Catalano, D. Bagetta, F. Mesiti, F. A. Ambrosio, I. Romeo, F. Moraca, R. Rocca, F. Ortuso, A. Artese, G. Costa, S. Alcaro and A. Lupia, “The Mediterranean Diet as source of bioactive compounds with multi-targeting anti-cancer profile,” *European Journal of Medicinal Chemistry,* vol. 181, 2019.

[41] M. S. Donaldson, “Nutrition and cancer: A review of the evidence for an anti-cancer diet,” *Nutrition Journal,* vol. 3, no. 19, 2004.

[42] “IHME, Global Burden of Disease, Our World in Data,” 2016. [Online]. Available: http://www.healthdata.org/gbd. [Accessed 8 March 2020].

[43] C. M. Lăcătușu, E. D. Grigorescu, M. Floria, A. Onofriescu and B. M. Mihai, “The Mediterranean Diet: From an Environment-Driven Food Culture to an Emerging Medical Prescription,” *International journal of environmental research and public health,* vol. 6, no. 16, 2019.

[44] V. D. Blondel, J.-L. Guillaume, R. Lambiotte and E. Lefebvre, “Fast unfolding of communities in large networks,” *J. Stat. Mech.,* 2008.

[45] M. Rosvall, D. Axelsson and C. T. Bergstrom, “The map equation,” *The European Physical Journal Special Topics,* vol. 178, no. 1, pp. 13-23, 2009.

[46] “Plotly: Modern Analytic Apps for the Enterprise,” Plotly, [Online]. Available: https://plot.ly/. [Accessed 8 March 2020].

[47] “Matplotlib: Python plotting,” Matplotlib, [Online]. Available: https://matplotlib.org/. [Accessed 8 March 2020].

[48] “seaborn: statistical data visualization,” Seaborn, [Online]. Available: https://seaborn.pydata.org/. [Accessed 8 March 2020].

[49] “Project Jupyter,” Jupyter, [Online]. Available: https://jupyter.org/. [Accessed 8 March 2020].

[50] I. T. Jolliffe and J. Cadima, “Principal component analysis: a review and recent developments,” *Philosophical Transactions of The Royal Society A Mathematical Physical and Engineering Sciences,* vol. 374, no. 2065, 2016.

[51] L. v. d. Maaten and G. Hinton, “Visualizing Data using t-SNE,” *Journal of Machine Learning Research,* vol. 9, pp. 2579-2605, 2008.

[52] A. Salvador, M. Drozdzal, X. Giro-i-Nieto and A. Romero, “Inverse Cooking: Recipe Generation from Food Images,” *Computer Vision and Pattern Recognition,* 2018.

[53] A. Salvador, N. Hynes, Y. Aytar, J. Marin, F. Ofli, I. Weber and A. Torralba, “Learning cross-modal embeddings for cooking recipes and food images,” *Computer Vision and Pattern Recognition,* 2017.

[54] A. Y. Ng, M. I. Jordan and Y. Weiss, “On spectral clustering: analysis and an algorithm,” *Proceedings of the 14th International Conference on Neural Information Processing Systems: Natural and Synthetic,* p. 849–856, 2001.

[55] J. R. Aunan, W. C. Cho and K. Søreide, “The Biology of Aging and Cancer: A Brief Overview of Shared and Divergent Molecular Hallmarks,” *Aging and disease,* vol. 8, no. 5, p. 628–642, 2017.

[56] T. Mikolov, K. Chen, G. Corrado and J. Dean, “Efficient Estimation of Word Representations in Vector Space,” *Proceedings of the International Conference on Learning Representations,* 2013.

[57] R. Řehůřek, “gensim: Topic modelling for humans,” [Online]. Available: https://radimrehurek.com/gensim/. [Accessed 8 March 2020].

[58] M. Chary, S. Parikh, A. F. Manini, E. W. Boyer and M. Radeos, “A Review of Natural Language Processing in Medical Education,” *The Western Journal of Emergency Medicine,* vol. 20, no. 1, 2019.

[59] “pandas,” [Online]. Available: https://pandas.pydata.org/. [Accessed 8 March 2020].